Effects of thermal spin fluctuations on the electronic properties of itinerant magnets

Surprises from ab initio calculations

Kirill Belashchenko

Department of Physics and Astronomy, University of Nebraska-Lincoln

SPICE Workshop on Computational Quantum Magnetism (May 2015)

Thermal spin fluctuations → Electrons → Properties (T)

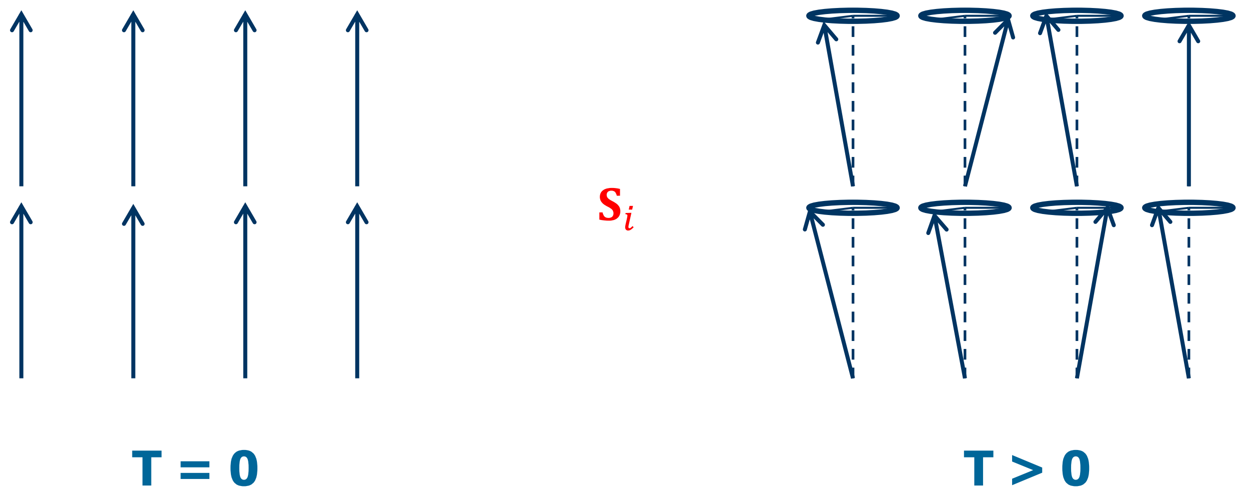

$$H_{\mathrm{SCF}} = H_0 - \frac{1}{2} I \sum_i \mathbf{S}_i \hat{\boldsymbol{\sigma}}_i$$

- ❖ Fluctuating spin moments polarize and scatter the conduction electrons
- ❖ T-dependent electronic spectrum, resistivity, magnetic anisotropy, etc.

Outline

- ❑ Magnetic anisotropy K(T) in $(Fe_{1-x}Co_x)_2B$ alloys
  - Thermal spin disorder can increase K(T)

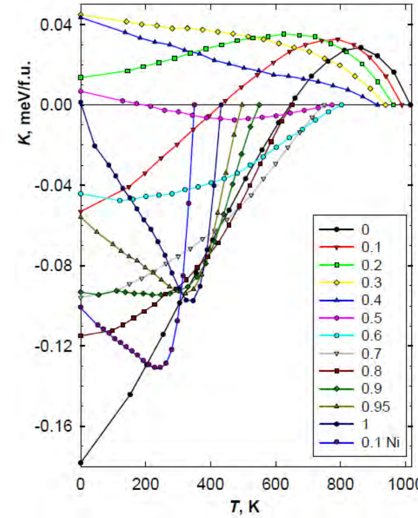

- ❑ Thermal depolarization of half-metallic NiMnSb
  - Dominant mechanism is due to Mn_{Sb} defects

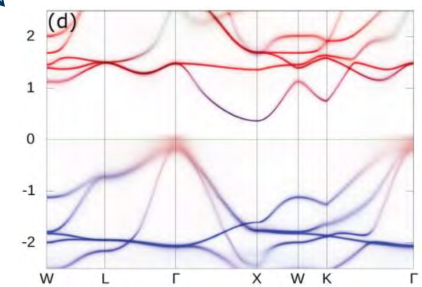

- ❑ Resistivity in rare-earths (spin fluct. + phonons)
  - Hidden resistivity saturation effect in Gd

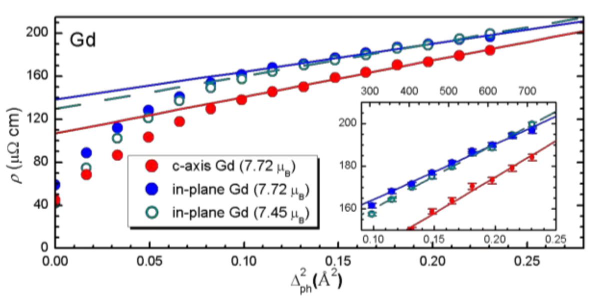

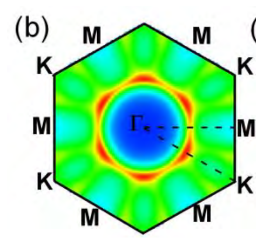

Methods

- Adiabatic approximation for spin fluctuations (static spin correlations)
- Coherent potential approximation (CPA) for chemical and spin disorder
- Disordered local moment (DLM) model of spin fluctuations ("static limit" of DMFT) (Oguchi et al, 1983; Gyorffy *et al.*, 1985)
    - Vector model (Staunton *et al.*, 2004) e.g. $p(\theta) \sim \exp(\alpha \cos \theta)$
    - Implemented in Green's function LMTO
    - Full charge self-consistency available, constraining fields
    - Spin-orbit coupling (perturbation of potential parameters)

"Components":

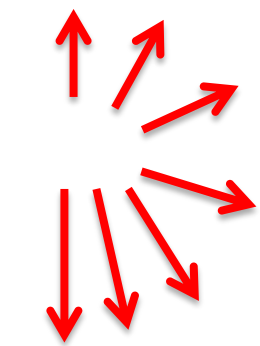

- Landauer-Büttiker method for transport calculations (supercell averaging over spin disorder)

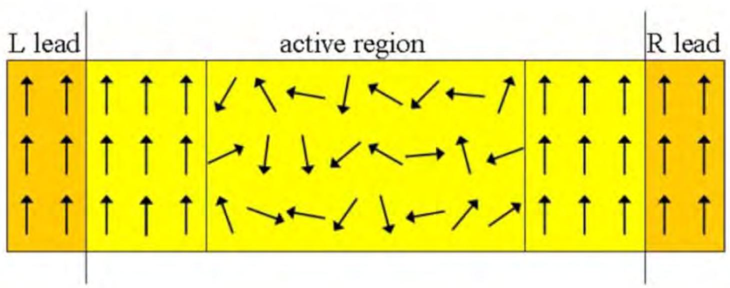

Anomalous T dependence of magnetic anisotropy

$(Fe_{1-x}Co_x)_2B$: exotic K(x,T), spin reorientations

Three spin reorientation transitions *vs* x

Anomalous temperature dependence

The Callen-Callen model gives: $K(T) \sim M^3(T)$ (single-site) or $M^2(T)$ (two-site) - monotonic

Known anomalies due to thermal expansion: hcp Co (Carr, 1958), MnBi

$(Fe_{1-x}Co_x)_2B$: anomalies due to spin fluctuations

First known case?

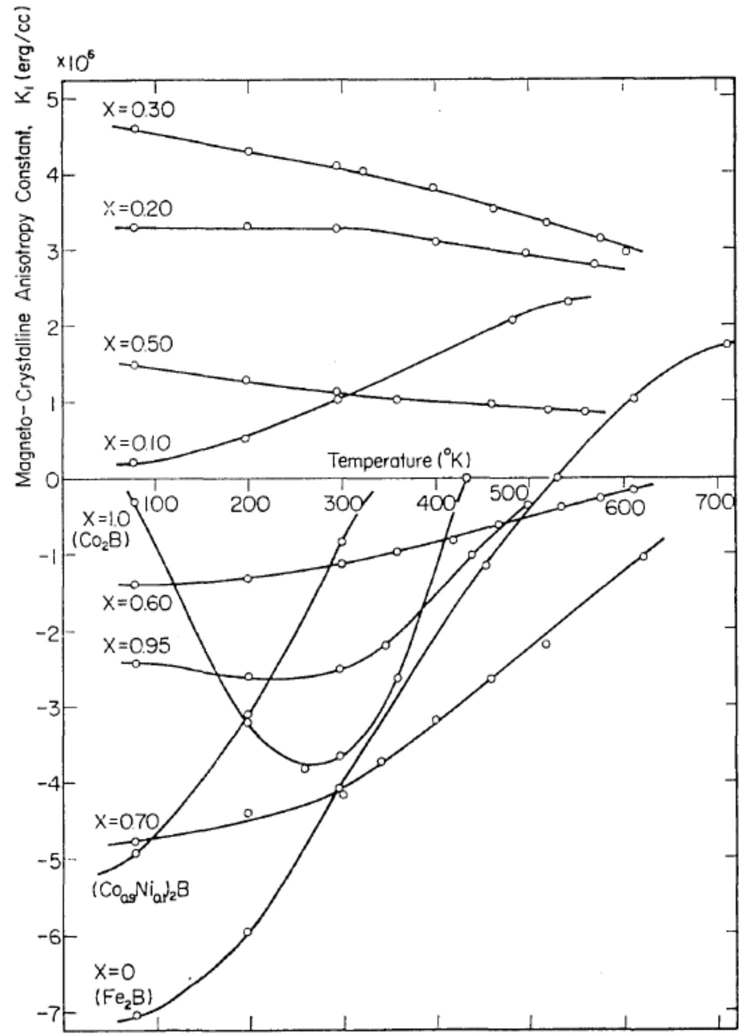

A. Iga, Jpn J. Appl. Phys. (1970)

Spin moments and magnetization

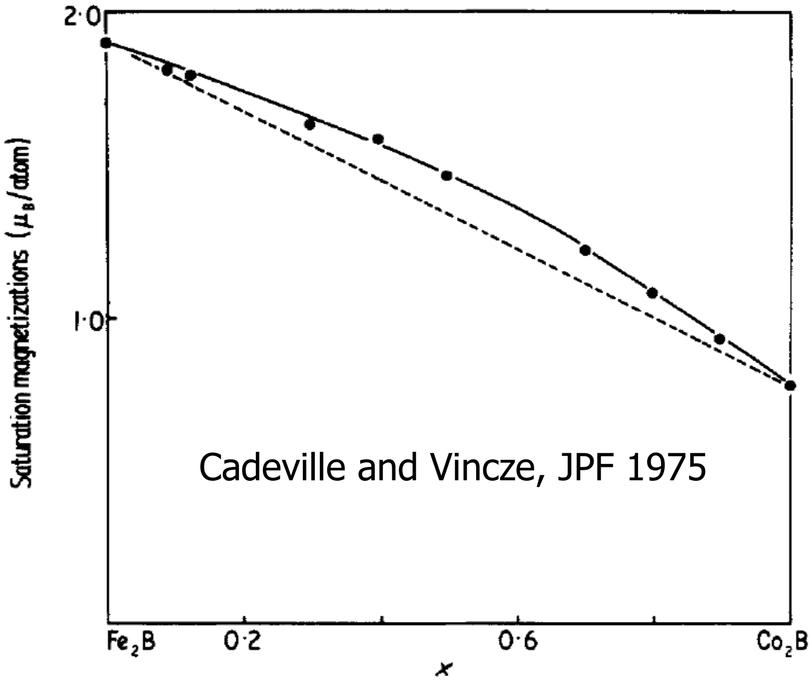

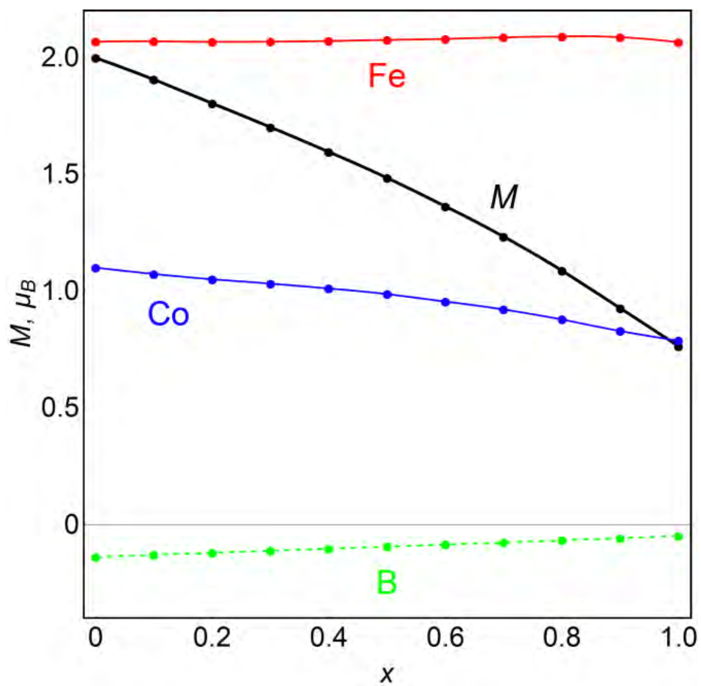

- Co spin moment is too large in DFT (LDA or GGA): 1.1 μ_B vs 0.76 μ_B (missing quantum spin fluctuations in DFT)
- Anisotropy is sensitive to exchange splitting (it affects band filling)

❖ Correction: Scale the B_{xc} field for Co by 0.8 everywhere

❖ Accelerated decline of the Co spin moment at x > 0.6 (agrees with expt)

Magnetocrystalline anisotropy, spin resolution

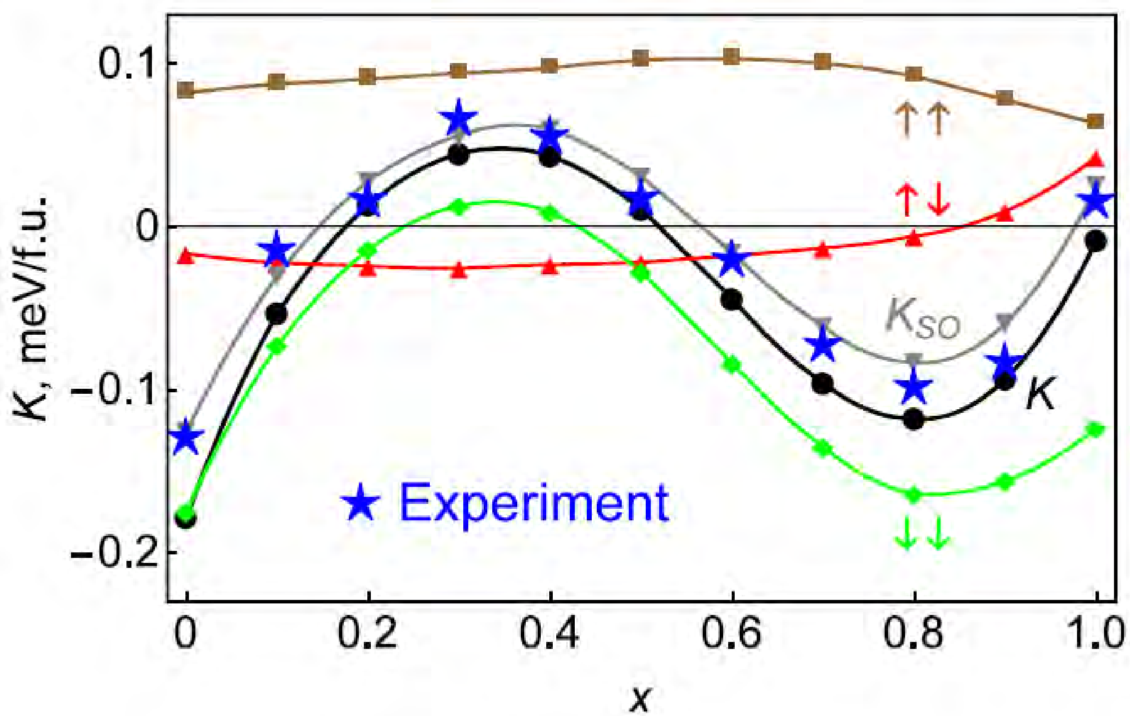

★ Experiment (2 K)

- Separation in spin channels (exact in 2nd order PT):

$$\Delta E_2 \approx \frac{1}{2}\langle H_{SO}\rangle = K_{SO} = K_{\uparrow\uparrow} + K_{\uparrow\downarrow} + K_{\downarrow\uparrow} + K_{\downarrow\downarrow}$$

- ❖ Spin-flip terms are small except near Co_2B
- ❖ $K_{\uparrow\uparrow}$ is positive and nearly constant; variation comes from $K_{\downarrow\downarrow}$

Brillouin zone map of MCA in Fe_2B (↓ spin)

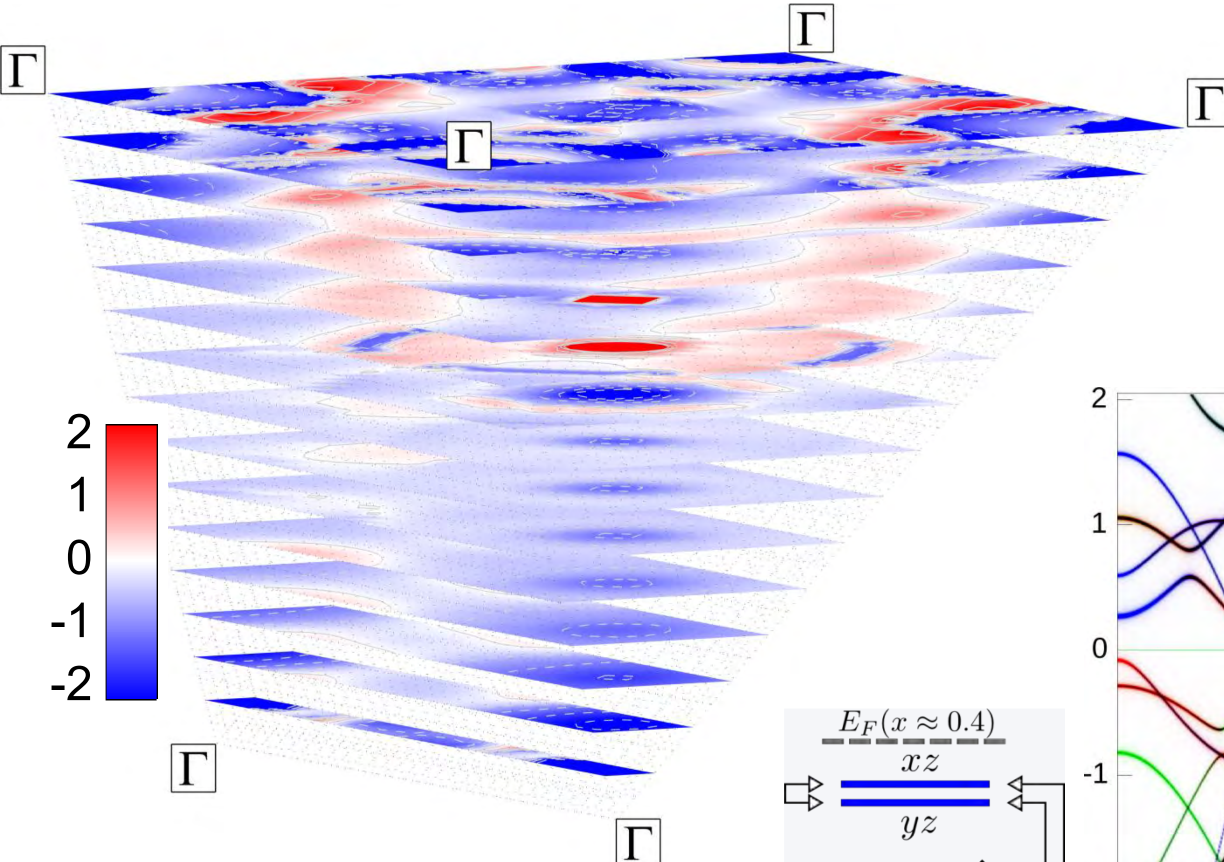

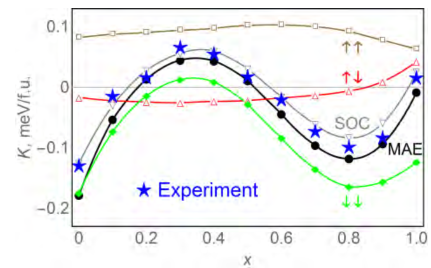

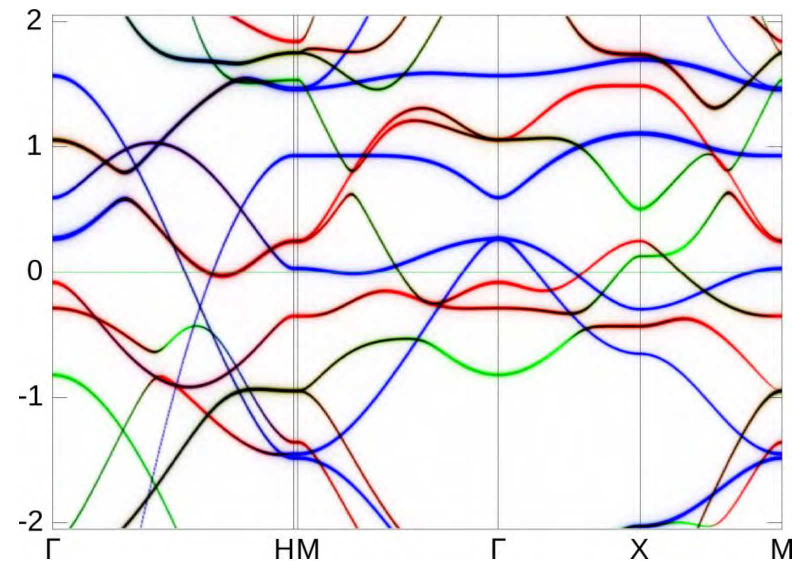

- Parity selection rule for $z \to -z$ on the ΓMX plane
- $\hat{L}_z$ even, $\hat{L}_x$ odd
- $\hat{L}_x$ couplings: in-plane MCA

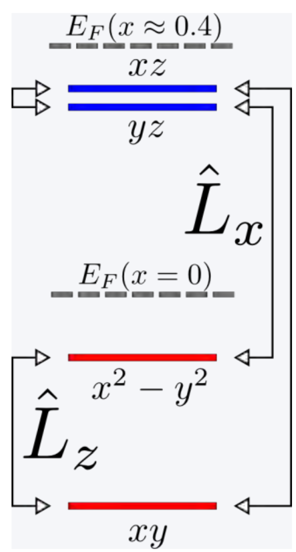

Red: xy and $x^2 - y^2$ (even, $m = \pm 2$)
Blue: xz and yz (odd, $m = \pm 1$)
Green: $3z^2 - r^2$ (even, $m = 0$)

MCA in $(Fe_{0.7}Co_{0.3})_2B$ (↓ spin)

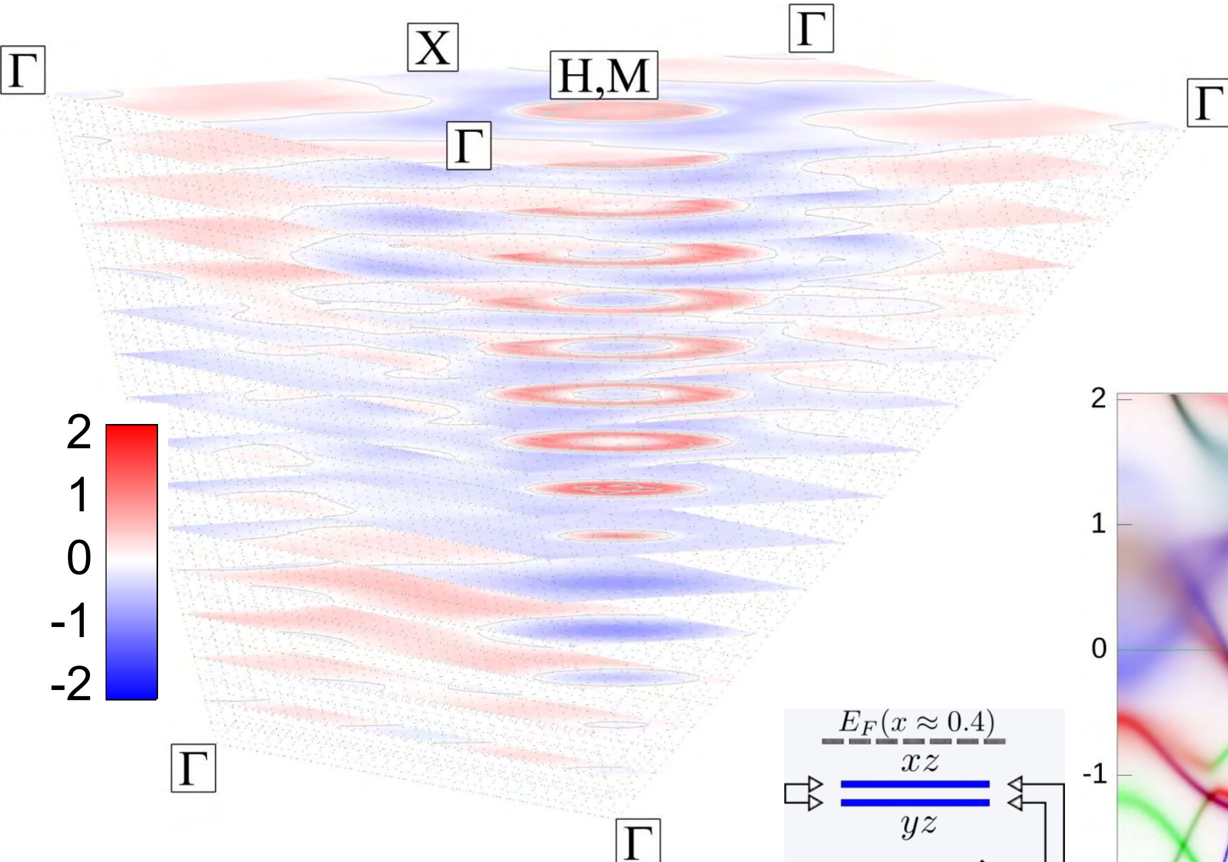

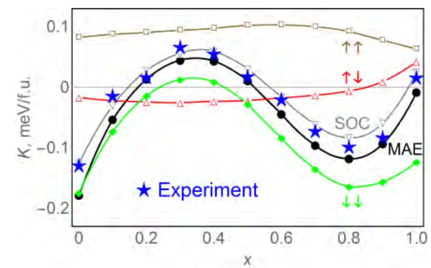

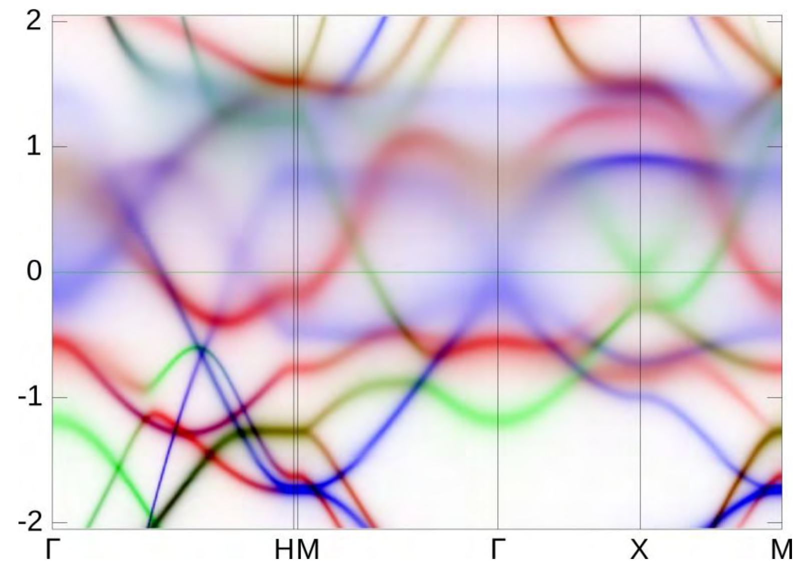

- xz, yz bands are filled
- Small MCA from spin ↓, spin ↑ dominates
- Band shifts + disorder

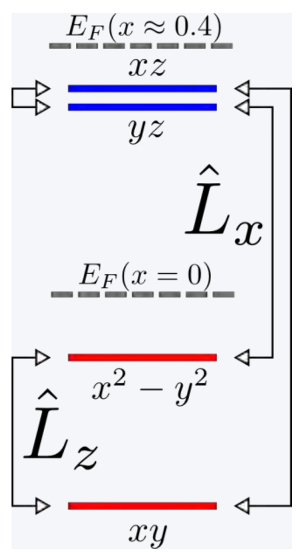

Red: xy and $x^2 - y^2$ (even, $m = \pm 2$)
Blue: xz and yz (odd, $m = \pm 1$)
Green: $3z^2 - r^2$ (even, $m = 0$)

MCA in $(Fe_{0.2}Co_{0.8})_2B$ (↓ only)

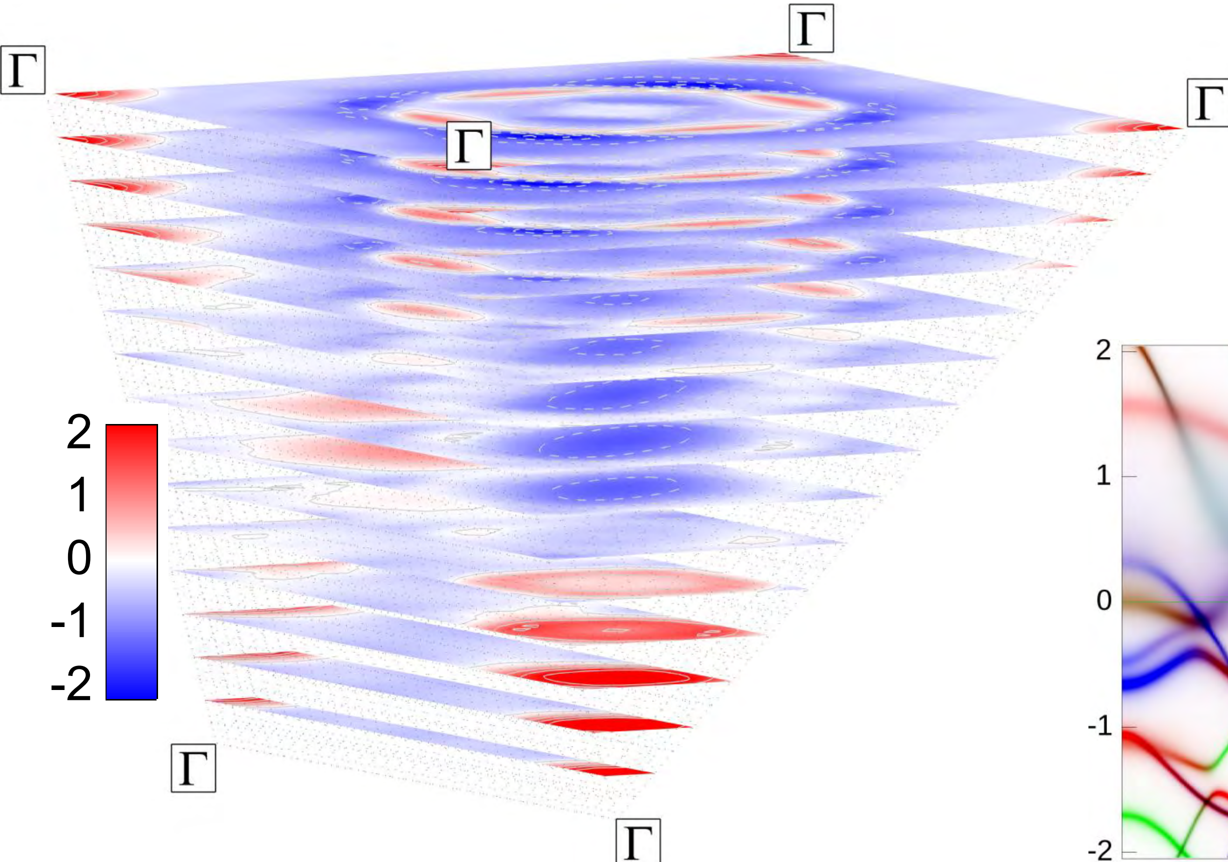

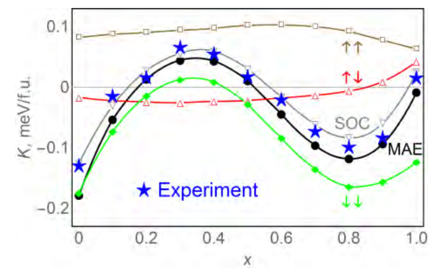

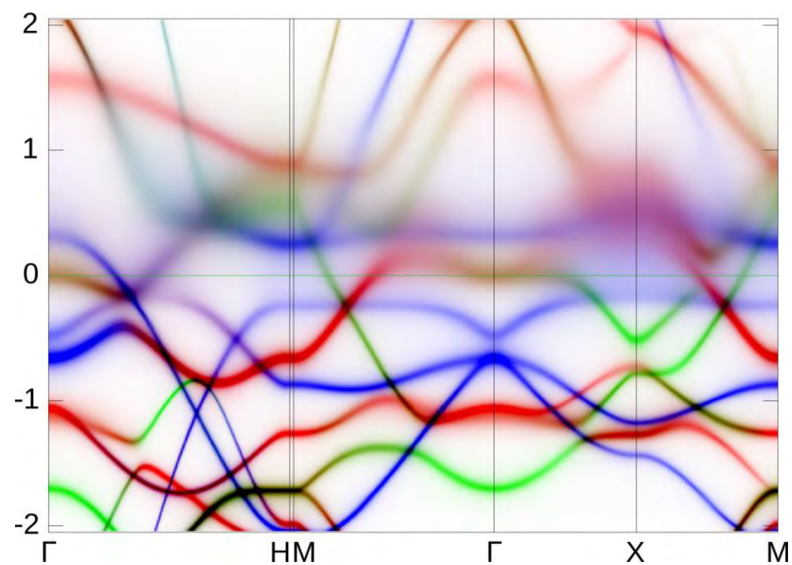

- Odd→even mixing: negative contribution
- Even doublet at E_F: split for M||z, positive contribution around Γ (reduced by disorder)
- Minimum of K(x) at $x = 0.8$

Red: xy and $x^2 - y^2$ (even, $m = \pm 2$)
Blue: xz and yz (odd, $m = \pm 1$)
Green: $3z^2 - r^2$ (even, $m = 0$)

❖ **Non-monotonic K(x): ↓ band filling, SO selection rules, disorder**

Temperature dependence of MCA

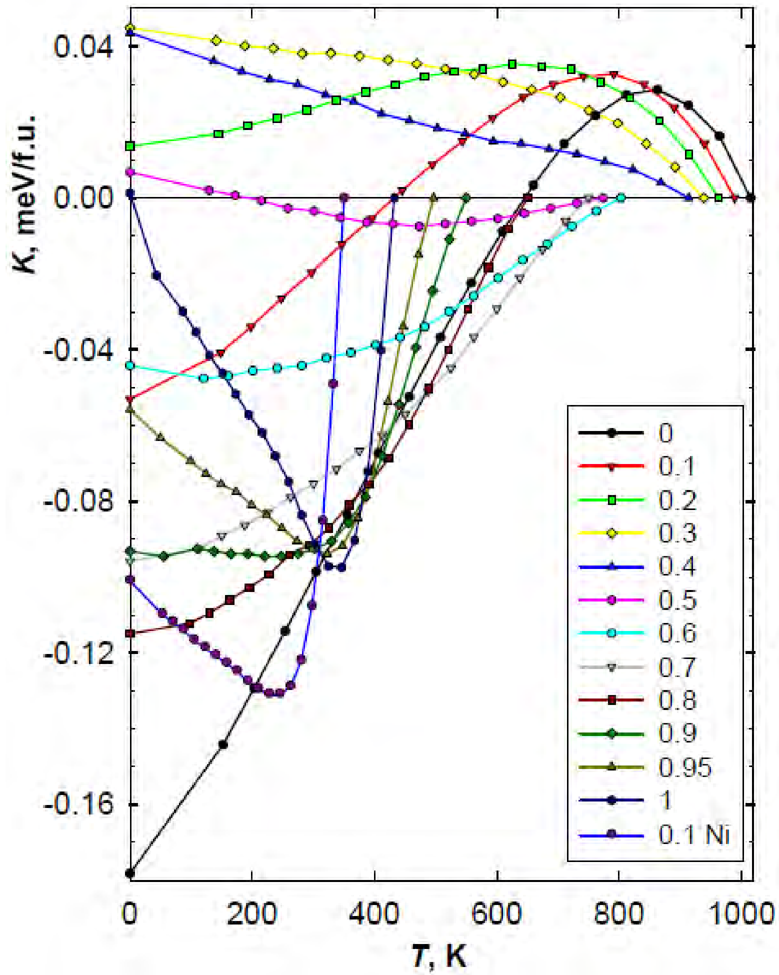

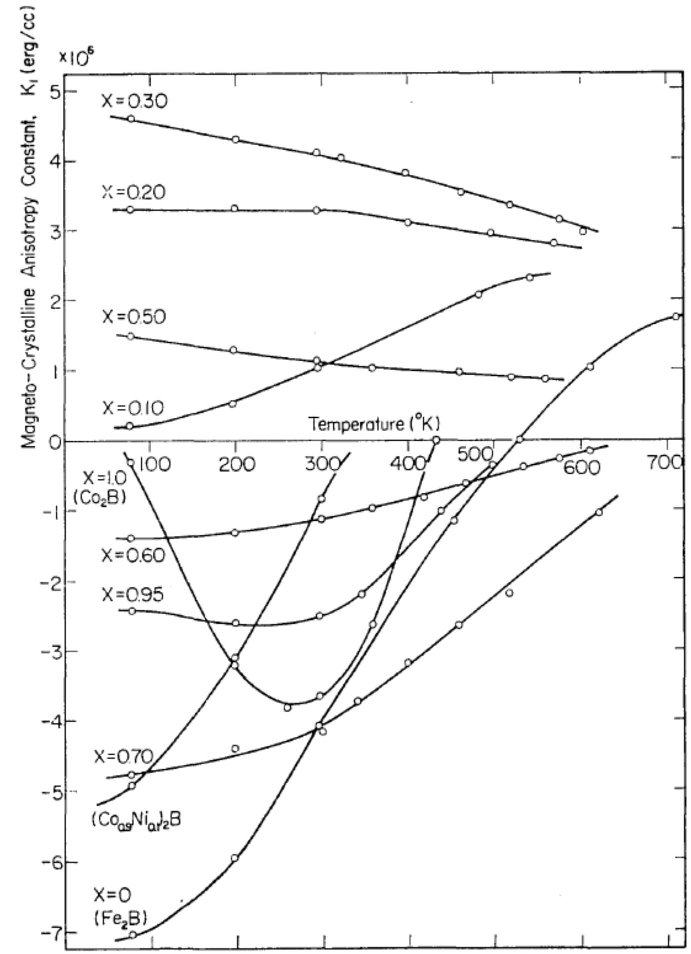

A. Iga, Jpn J. Appl. Phys. (1970)

- ❖ Excellent agreement with experiment
- ❖ Anomalous temperature dependence from spin fluctuations

Electronic structure at elevated T (with SOC)

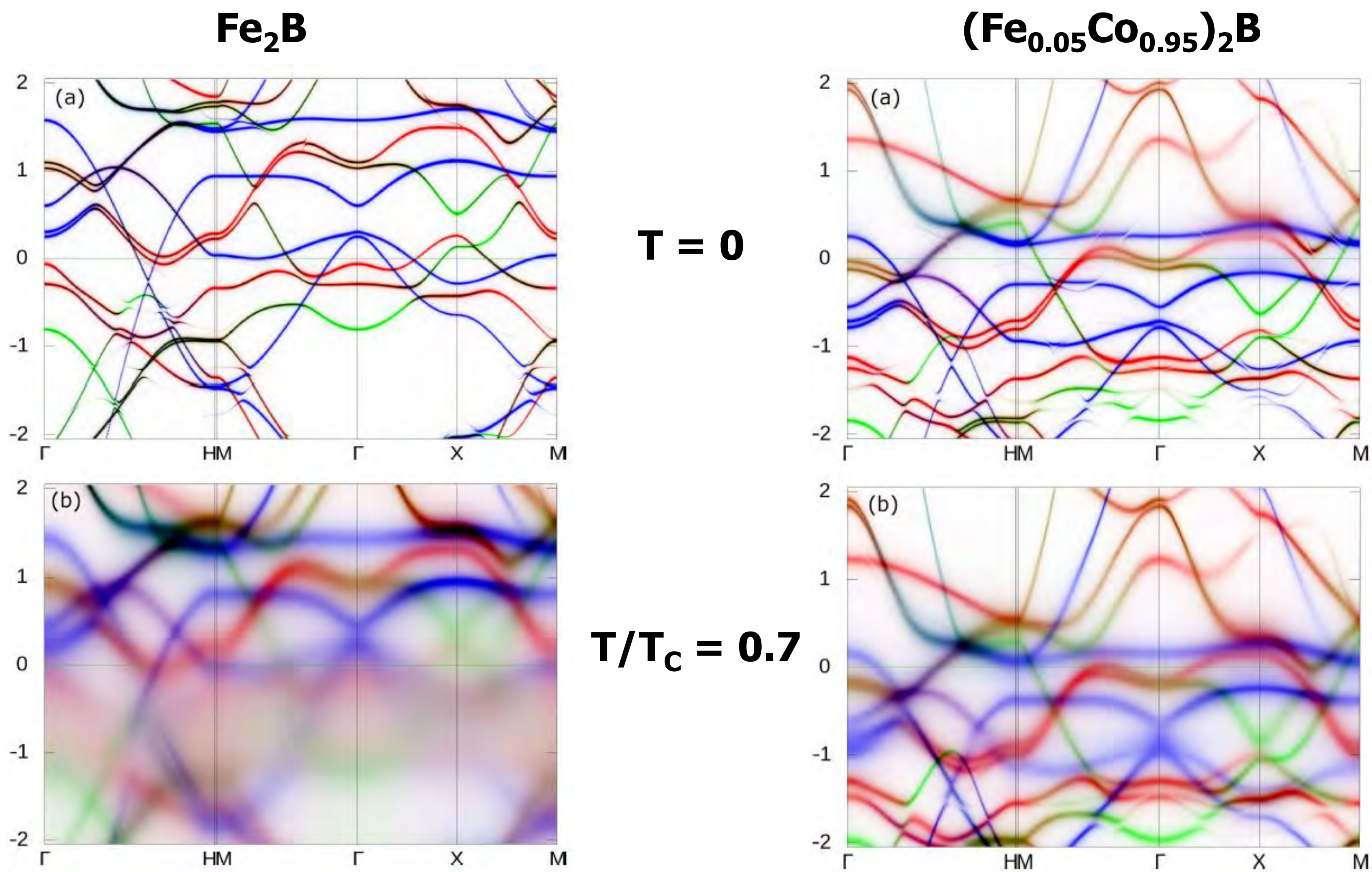

- ❖ Strong broadening at Fe-rich end, Stoner-like at Co-rich end
- ❖ Spin fluctuations affect MCA through disorder and band shifts

Effect of disorder on magnetic anisotropy

Virtual crystal vs CPA

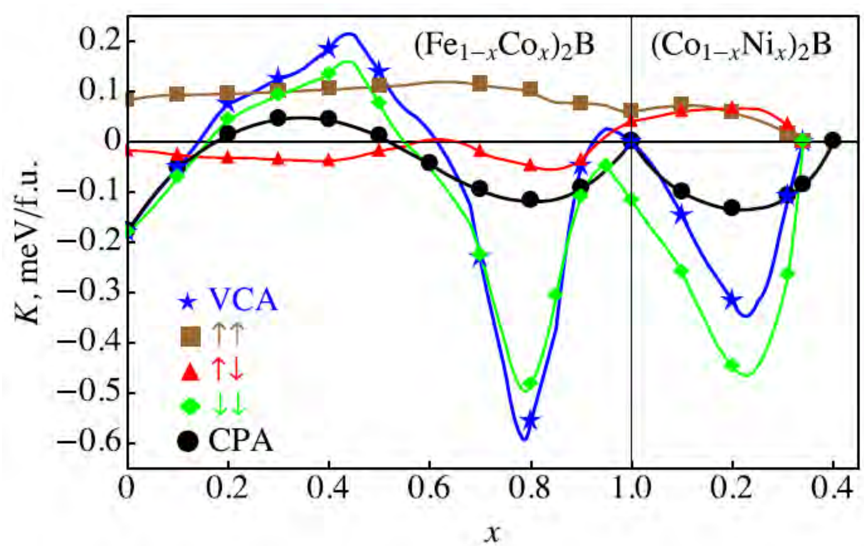

❖ Reduced ↓↓ term (flat bands near E_F)

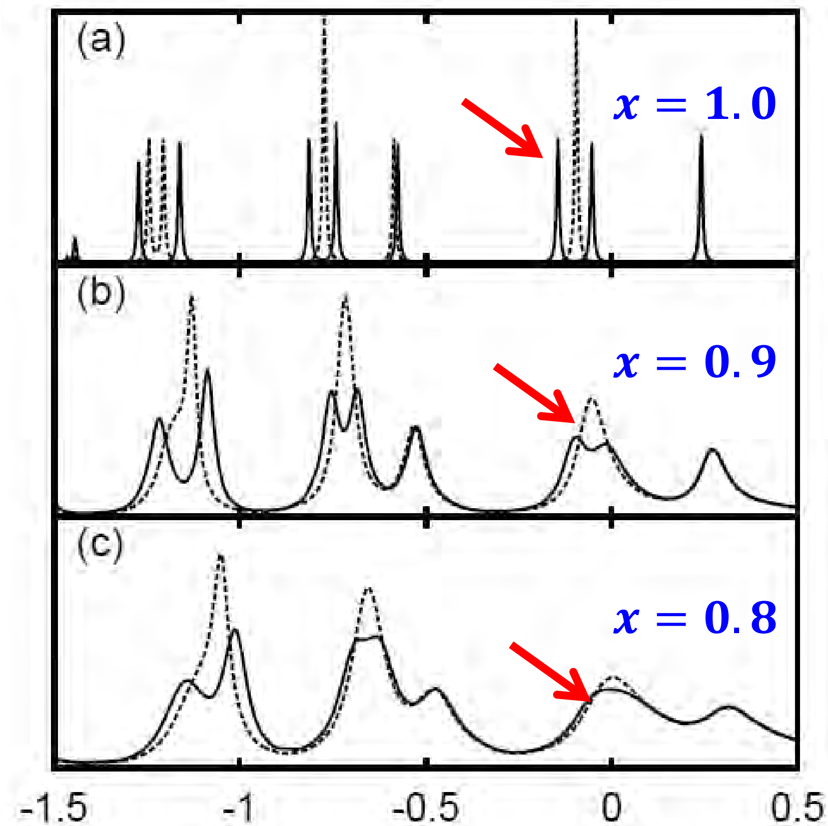

❖ Disorder suppresses "hot spots" from degenerate bands at E_F

❖ **Disorder does not uniformly suppress all MCA contributions**

Temperature dependence of MCA

Fe_2B

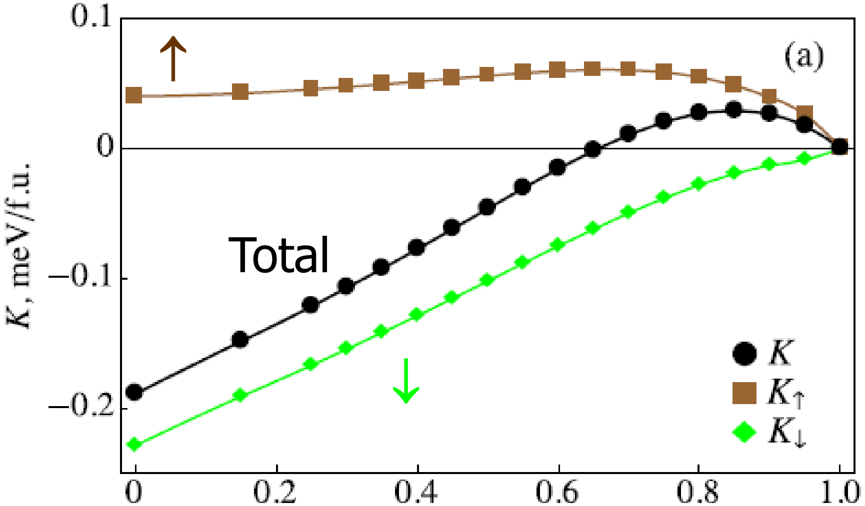

- $K_\downarrow$ suppressed by disorder
- $K_\uparrow$ grows due to band filling
- Spin reorientation transition

❖ Anomalous $K(T)$ through band broadening, Stoner band shifts

KB *et al.*, APL 106, 062408 (2015)
Zhuravlev *et al.*, arXiv:1503.04790

$(Fe_{0.05}Co_{0.95})_2B$

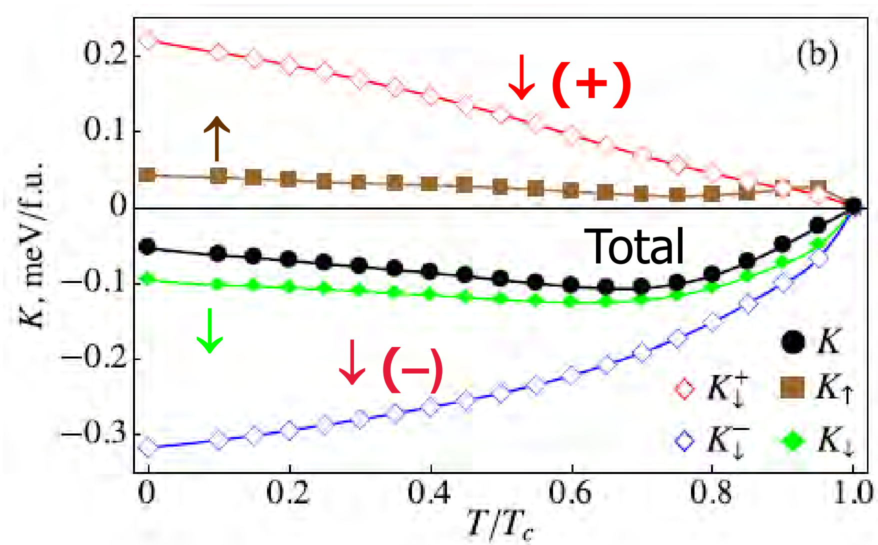

- "Hot spot" near Γ suppressed in $K_\downarrow$
- Non-monotonic $K(T)$

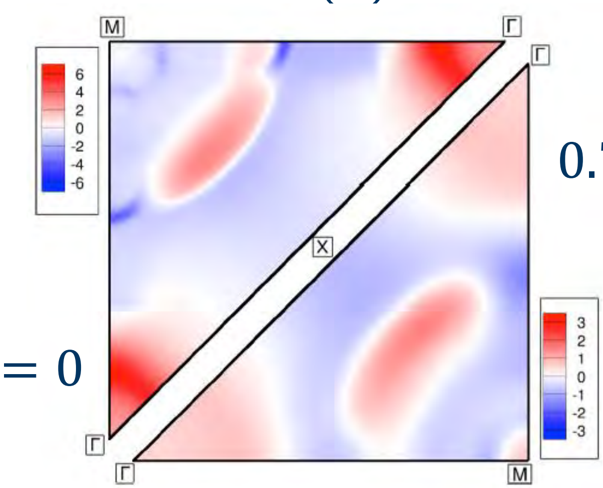

$0.7T_C$

$T = 0$

Thermal depolarization of a half-metallic ferromagnet

Half-metallic ferromagnet at finite T

- Ideally 100% polarization at the Fermi level
- Case study: **NiMnSb** (half-Heusler alloy)
- Low-T anomaly in resistivity

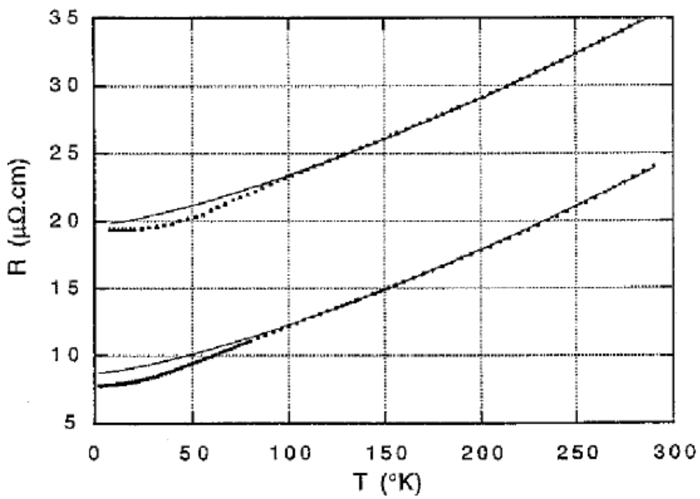

Hordequin *et al.*, JMMM 1996
Borca *et al.*, PRB 2001

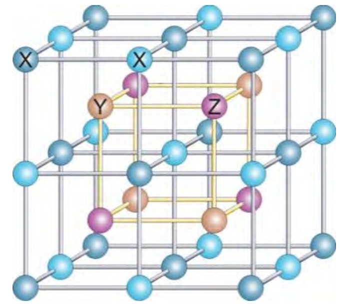

X_2YZ: full Heusler
XYZ: half-Heusler

Anomaly linked to excess Mn

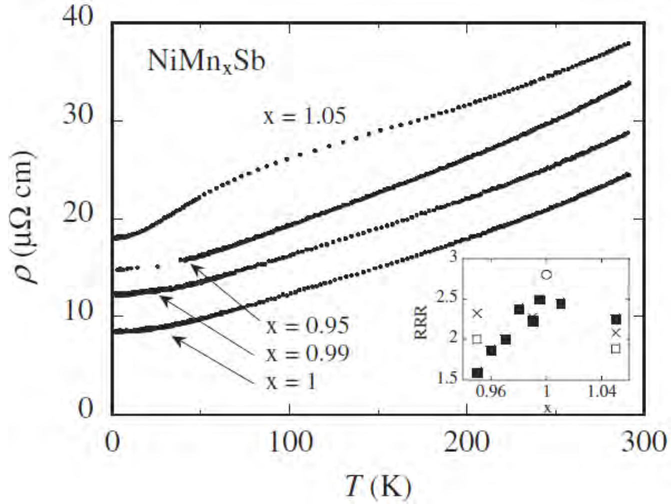

Wang *et al.*, Jpn J Appl Phys 2010

Evolution of NiMnSb spectral function with temperature

T = 0

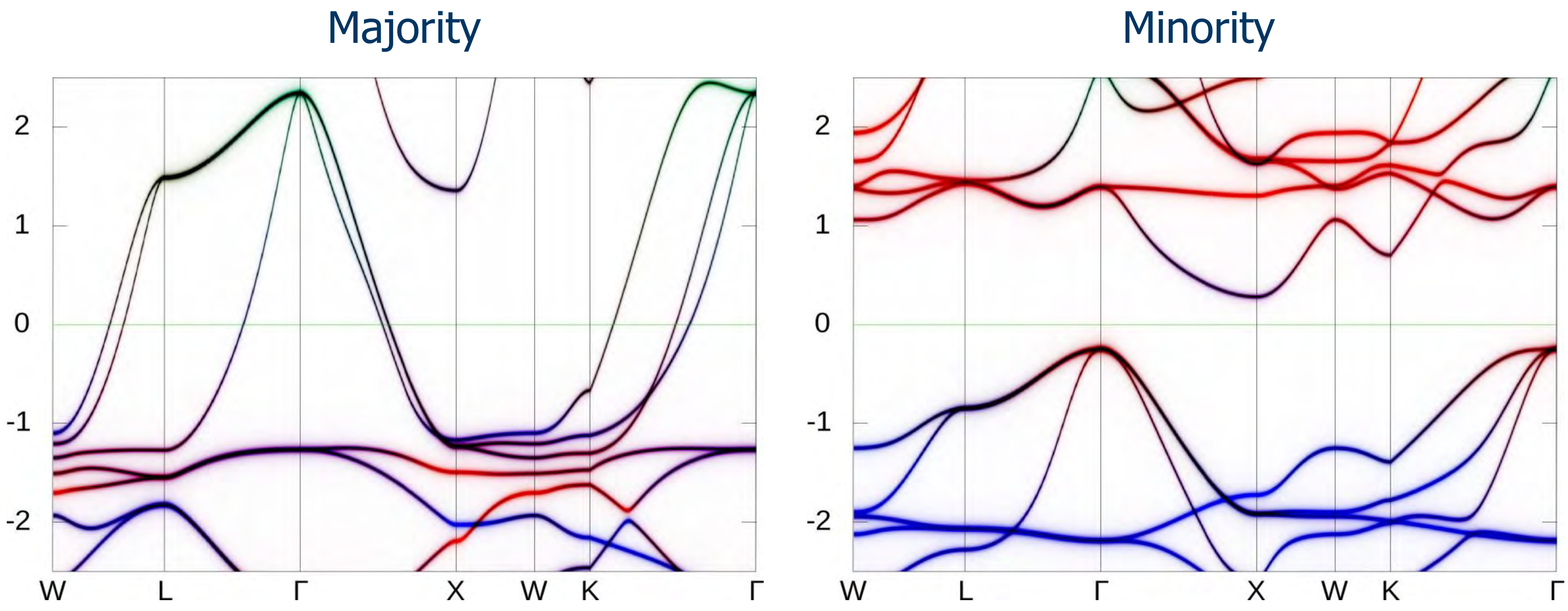

Color scheme: Ni Mn Sb

- ❖ Regular band structure at T = 0

Evolution of NiMnSb spectral function with temperature

T = 167 K

Majority | Minority

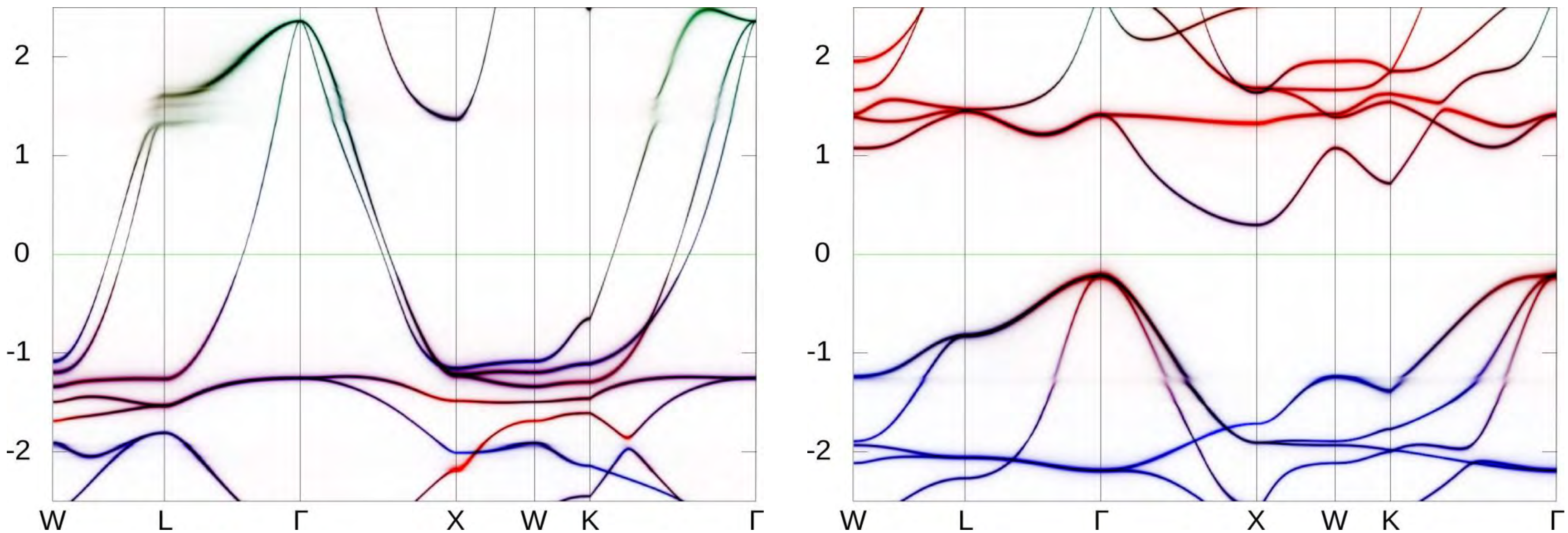

Color scheme: Ni Mn Sb

Evolution of NiMnSb spectral function with temperature

T = 257 K

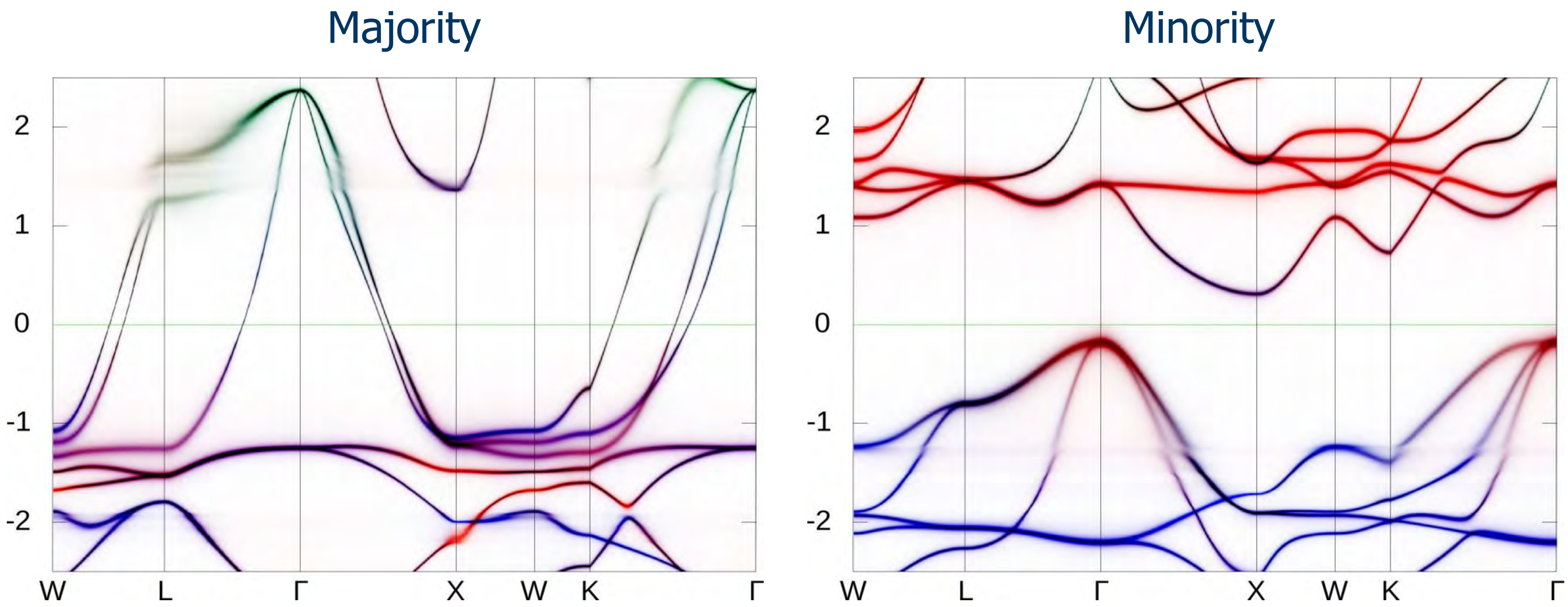

Color scheme: Ni Mn Sb

Evolution of NiMnSb spectral function with temperature

T = 399 K

Majority   Minority

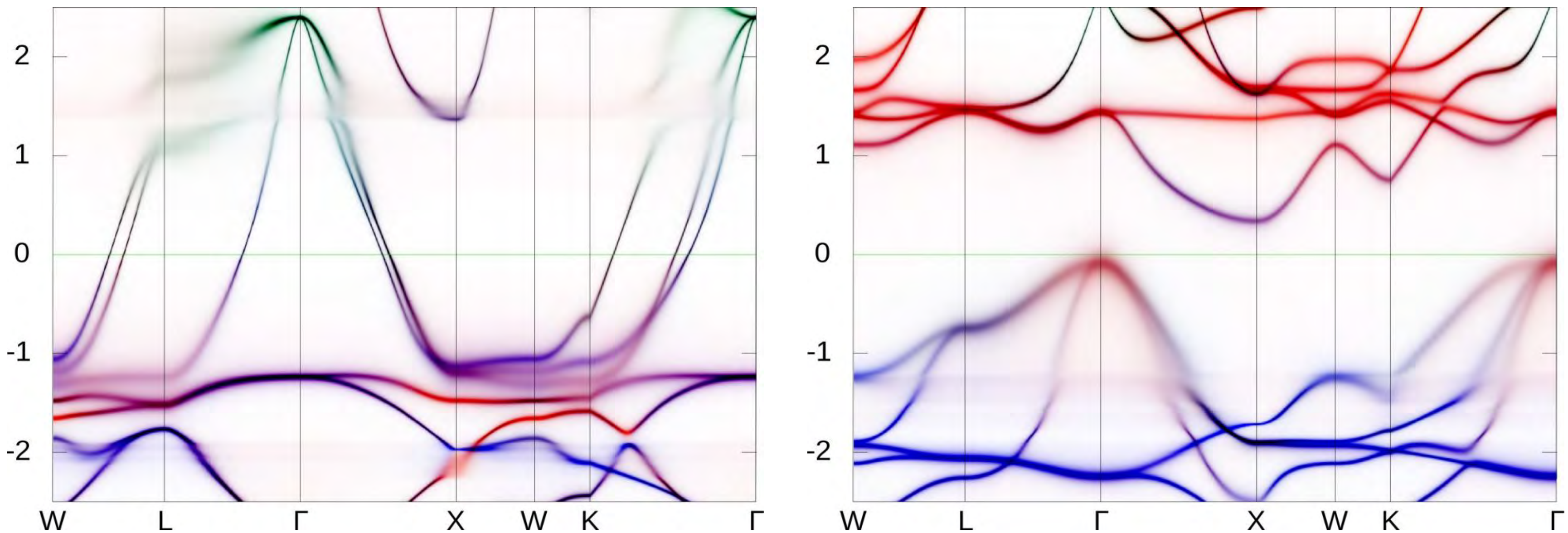

Color scheme: Ni Mn Sb

- Crossover to conventional ferromagnet (raising VBM at Γ)
- Negligible “shadow weight” from dispersive majority-spin bands

Evolution of NiMnSb spectral function with temperature

T = 490 K

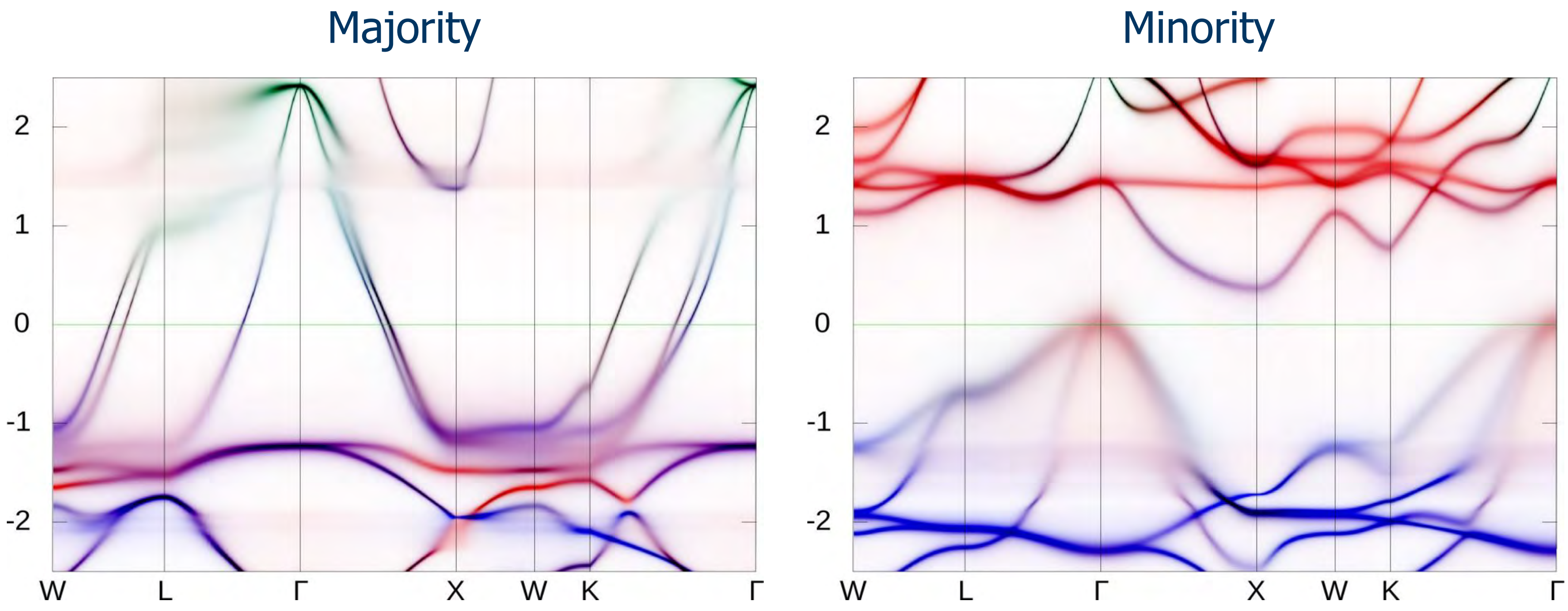

Color scheme: Ni Mn Sb

Evolution of NiMnSb spectral function with temperature

T = 586 K

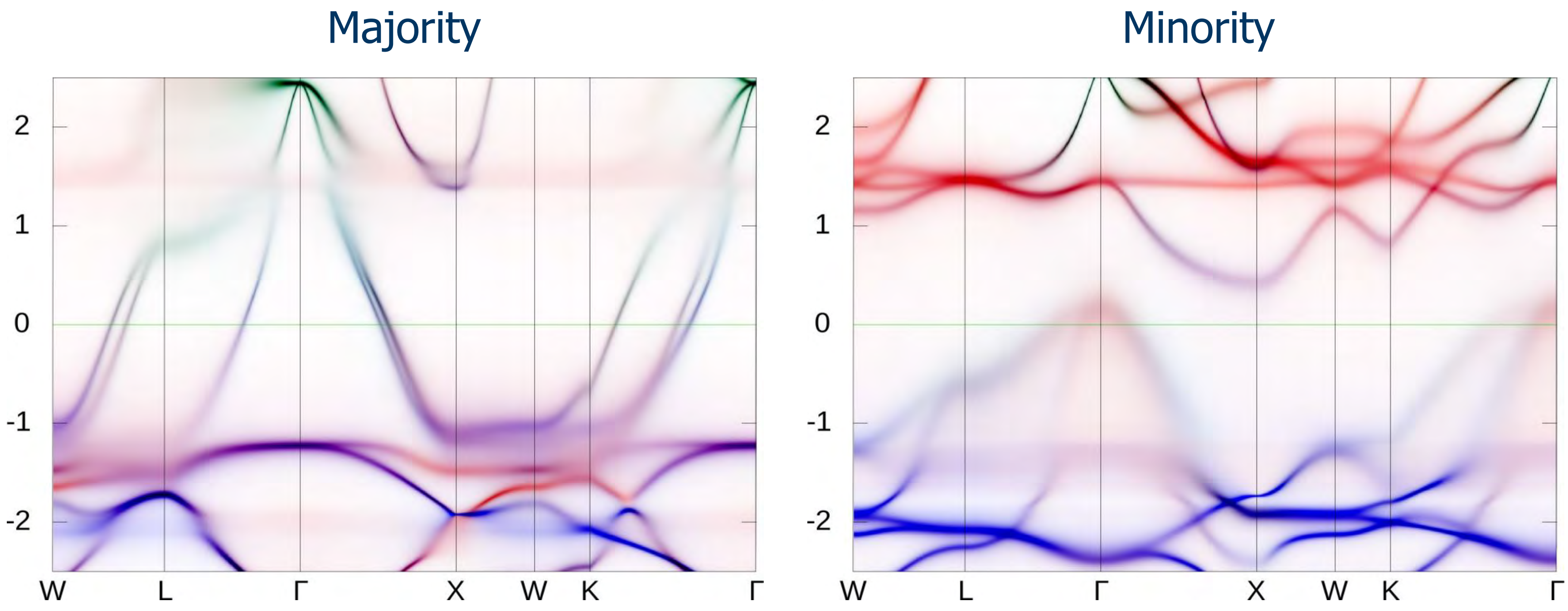

Color scheme: Ni Mn Sb

Ideal NiMnSb: VBM moves up at finite T, half-metallic gap persists up to ~400 K

Hybridization analysis

Mn t_{2g}
Mn e_g
(Sb states removed)

Sb (Mn,Ni 3d states removed)

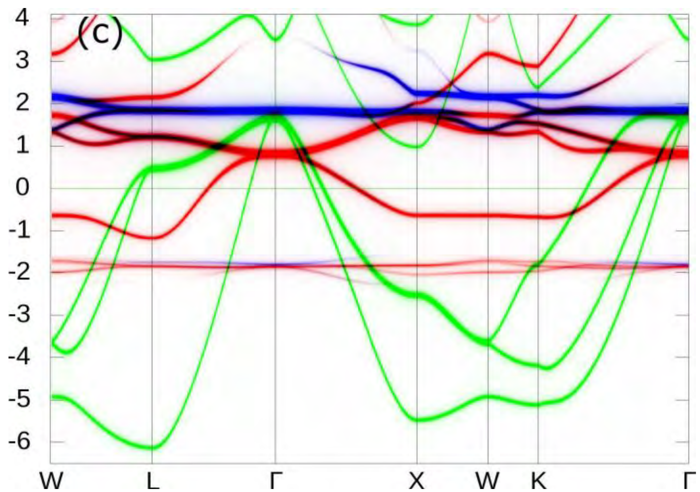

M/M_0=0.8

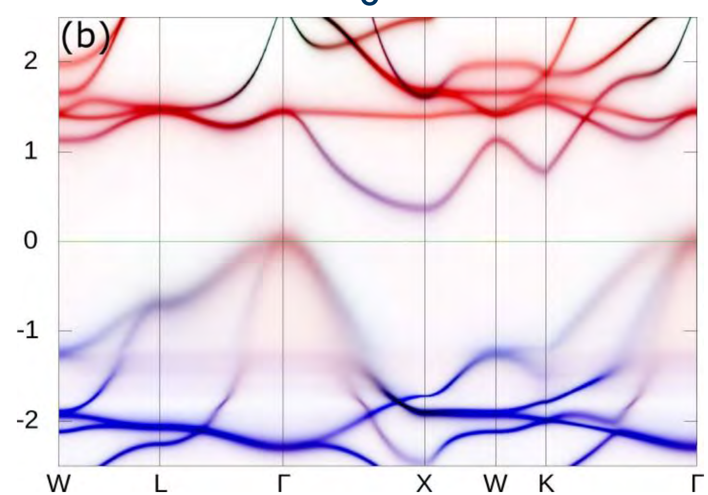

VBM and CBM: energy and width

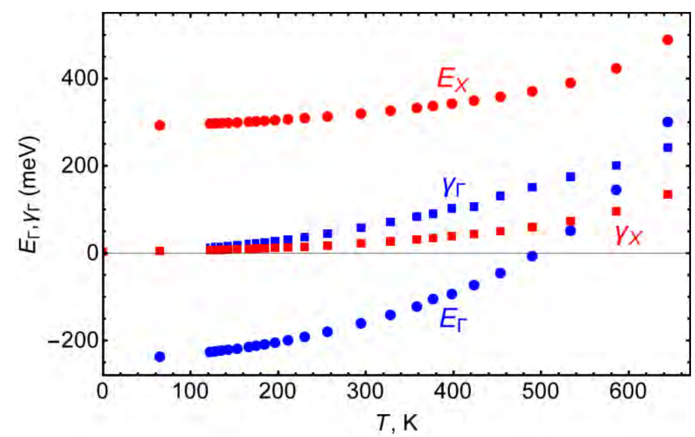

- VBM moves up with T due to unmixing of Mn t_{2g} states from Sb
- Crossover to conventional FM around 400 K

Excess Mn: exchange coupling to bulk

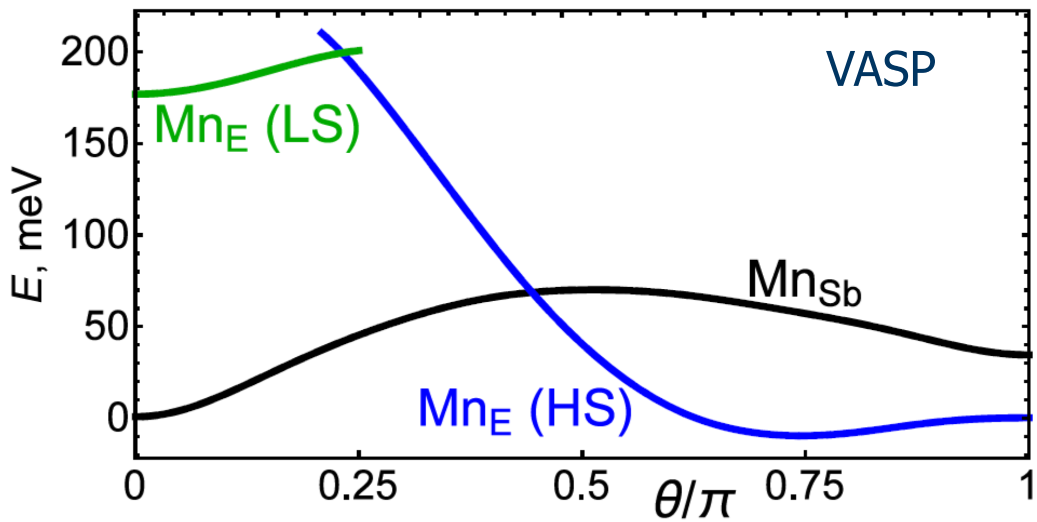

Host Mn atoms:
$E(\pi) = 730$ meV

- ❖ Mn_E, Mn_{Sb} weakly coupled to bulk **M**, disorder at low T
- ❖ Collinear Mn_E ($\theta = 0$), Mn_E ($\theta = \pi$), Mn_{Ni}, Mn_{Sb} preserve the gap
  (cf. Alling *et al.*, PRB 2006)

Mn_E with spin disorder (6.25%)

Mn_E spin ↑↓ to bulk **M**

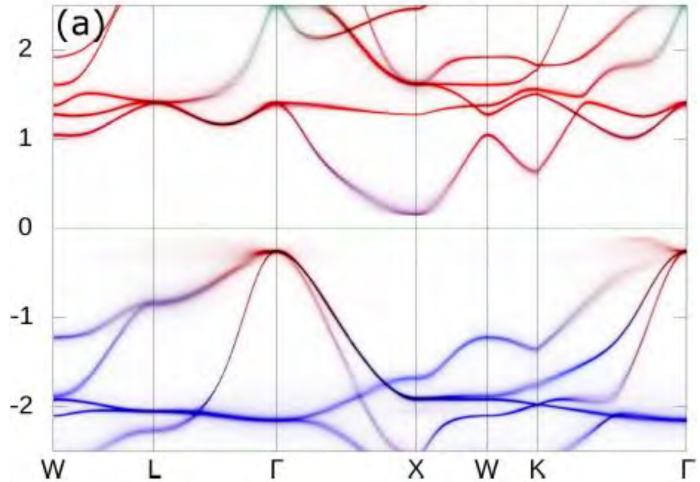

Disordered spins on Mn_E

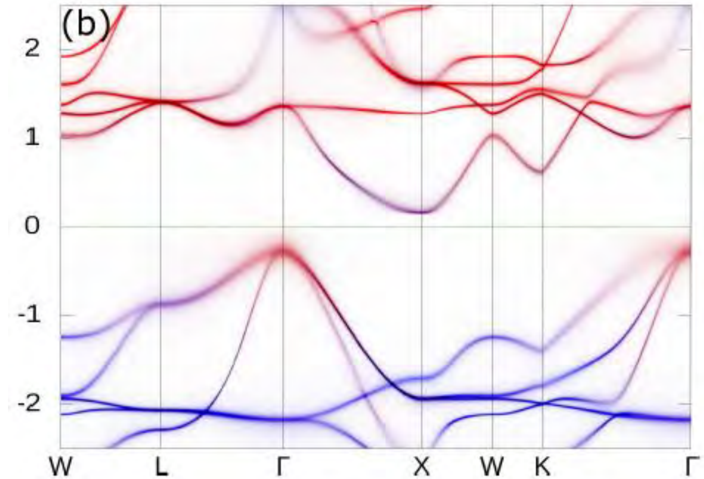

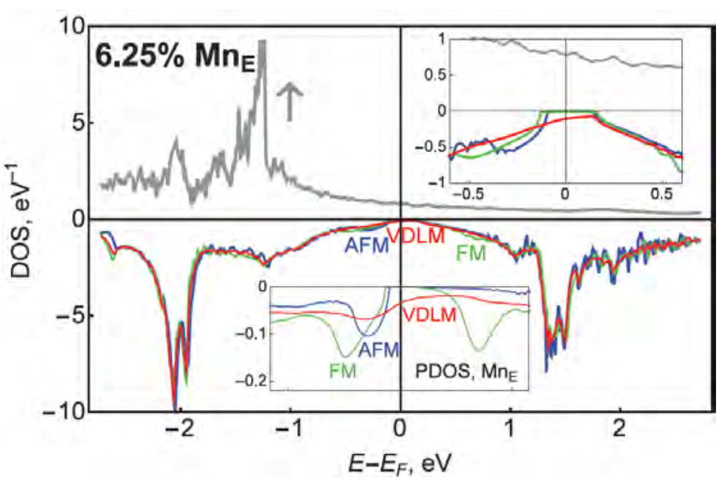

❖ Spin disorder on Mn_E broadens VBM, but changes at E_F are not large

Mn_{Sb} with spin disorder

Mn_{Sb} spin ↑↑ to bulk **M**

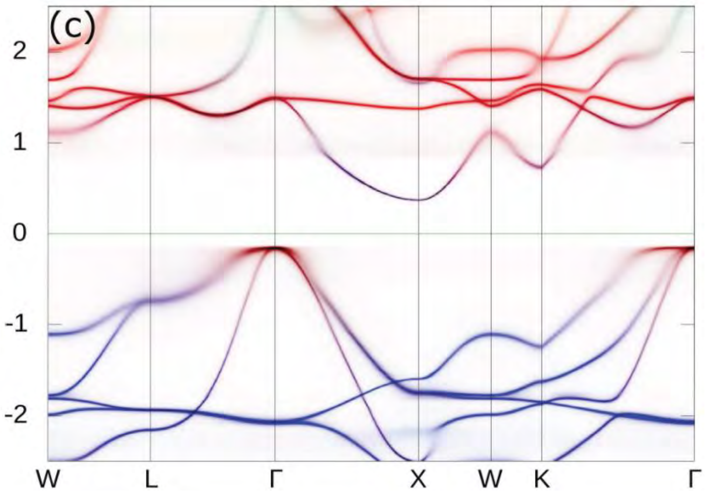

Fully disordered Mn_{Sb} spins

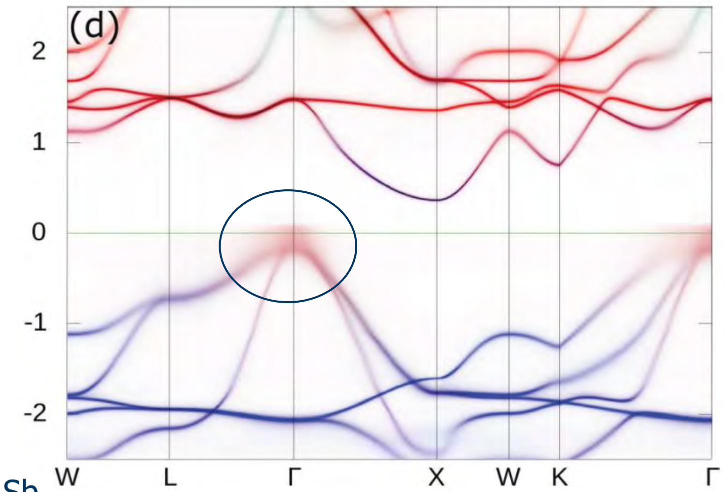

6.25% Mn_{Sb}

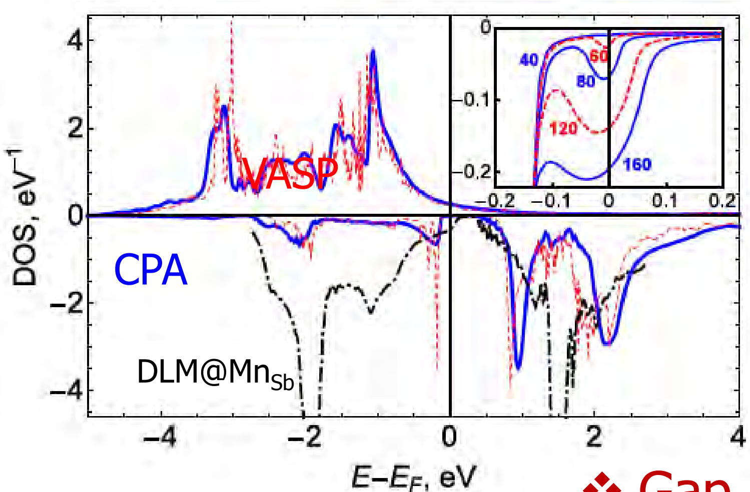

Spin polarization at E_F

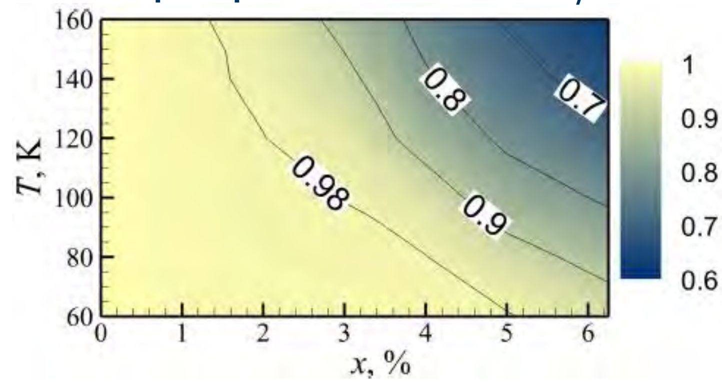

❖ Gap is destroyed by spin disorder on Mn_{Sb}
❖ Likely source of low-T anomaly

KB *et al.*, PRB(R) 2015, in press (arXiv:1501.00969)

Defects in NiMnSb: Experimental data

Polarized neutron diffraction [Brown et al., JPCM **22**, 206004 (2010)]

NiMnSb (A): grain growth, annealed 60 days in Ar at 1000°C
NiMnSb (B): Bridgeman technique

Site		PdMnSb	NiMnSb (A)	NiMnSb (B)
A	b (fm)	−2.62(2)	−3.73(4)	−2.60(4)
	Occ (%)	Mn 85(8) Sb 10(1)	Mn 100.0(5)	Mn 87.5(5) Sb 11.7(5)
	μ (μ_B)	4.52(3)	4.11(5)	3.98(4)
B	b (fm)	4.62(2)	5.33(4)	4.20(4)
	Occ (%)	Sb 90.0(2) Mn 9.4(9)	Sb 95.5(4)	Sb 81.6(6) Mn 12.5(5)
	μ (μ_B)	0	0	3.98(4)
C	b (fm)	5.68(5)	10.39(4)	9.00(12)
	Sb (%)	Pd 95.0(5) Mn 5.0(5)	Ni 100.0(3)	Ni 85(2) Sb 6(1)
	μ (μ_B)	0	0.15(2)	0.05(4)
D	b (fm)	0.03(5)	0.14(4)	9.00(12)
	(%)	Pd 0.5(8) Mn 0.0(1)	Ni 1.6(3)Sb 0.2(1)	Ni 15(2) Sb 1(1)
	μ (μ_B)	0	0	1.0(3)

❖ Mn/Sb (B2 type) disorder and Ni_E in lower-quality sample B

Spin disorder resistivity in rare earth metals

Spin-disorder resistivity

- Scattering on spin fluctuations – no *ab initio* results until recently

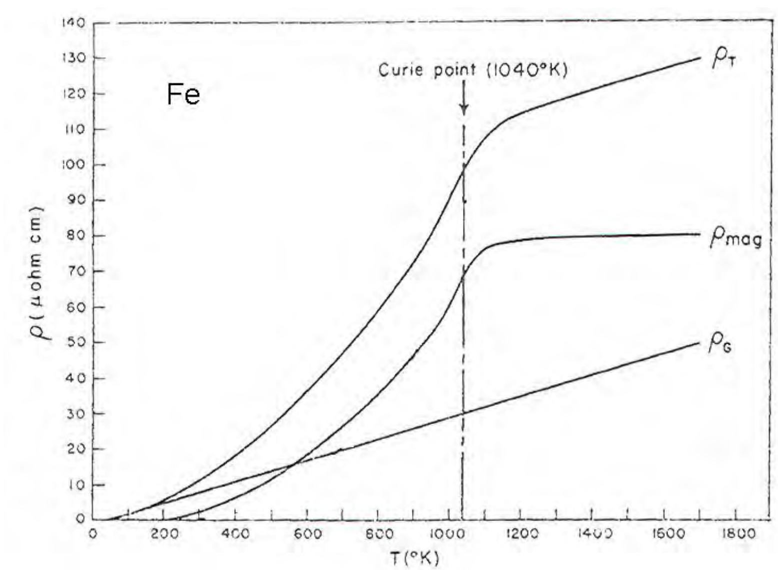

Weiss and Marotta, 1959

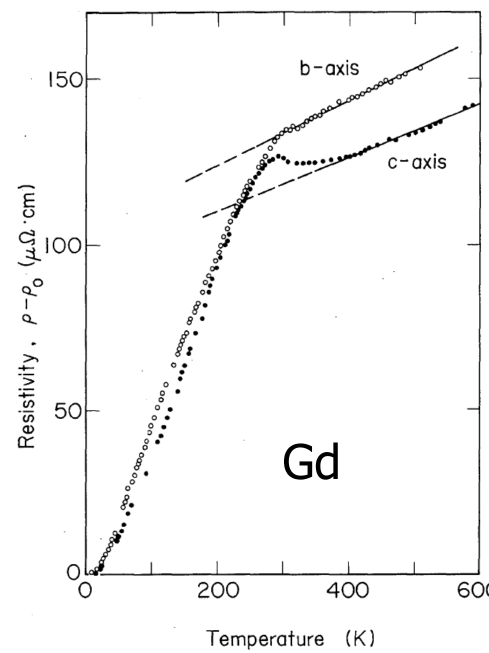

Maezawa *et al.*, JPSJ 1977

Calculations for Fe and Ni: see Wysocki, KB *et al.* (PRB 2009)

Spin-disorder resistivity of rare earths

f-d model prediction (mean-field approximation):

$\rho_{\text{PM}} \propto J_{fd} S(S+1)$, weak spin-orbit

$\rho_{\text{PM}} \propto J_{fd} (g-1)^2 J(J+1)$, strong spin-orbit

Kasuya, 1956
De Gennes, 1958
Brout and Suhl, 1959

S. Legvold, PRB 3, 1640 (1971)

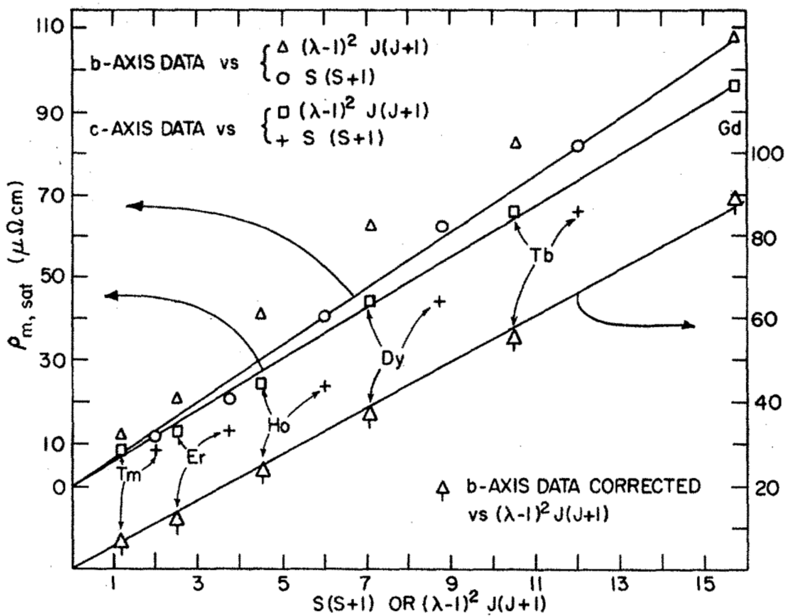

	Gd	Tb	Dy	Ho	Er	Tm	Lu
$\frac{d\rho_b}{dT}$ ($T \gtrsim$ 300 K)	0.095	0.13	0.15	0.185	0.20	0.22	0.25
$\frac{d\rho_c}{dT}$ ($T >$ 300 K)	0.08	0.085	0.09	0.11	0.11	0.12	0.12

de Gennes factor $(g-1)^2 J(J+1)$

- Raw data: $(g-1)^2 J(J+1)$ for *c*-axis; *S*(*S*+1) for in-plane
- Rescaling based on dρ/dT above T_c (assumes large FS changes, contradicts *ab initio* data)

$$\int v_\alpha^2 \delta(E-E_F) d\mathbf{k}$$

Element	In-plane	*c*-axis
Gd	0.679	1.247
Tb	0.655	1.257
Dy	0.609	1.217
Ho	0.571	1.166
Er	0.548	1.135
Tm	0.532	1.108

Resistivity vs (exchange splitting)^2

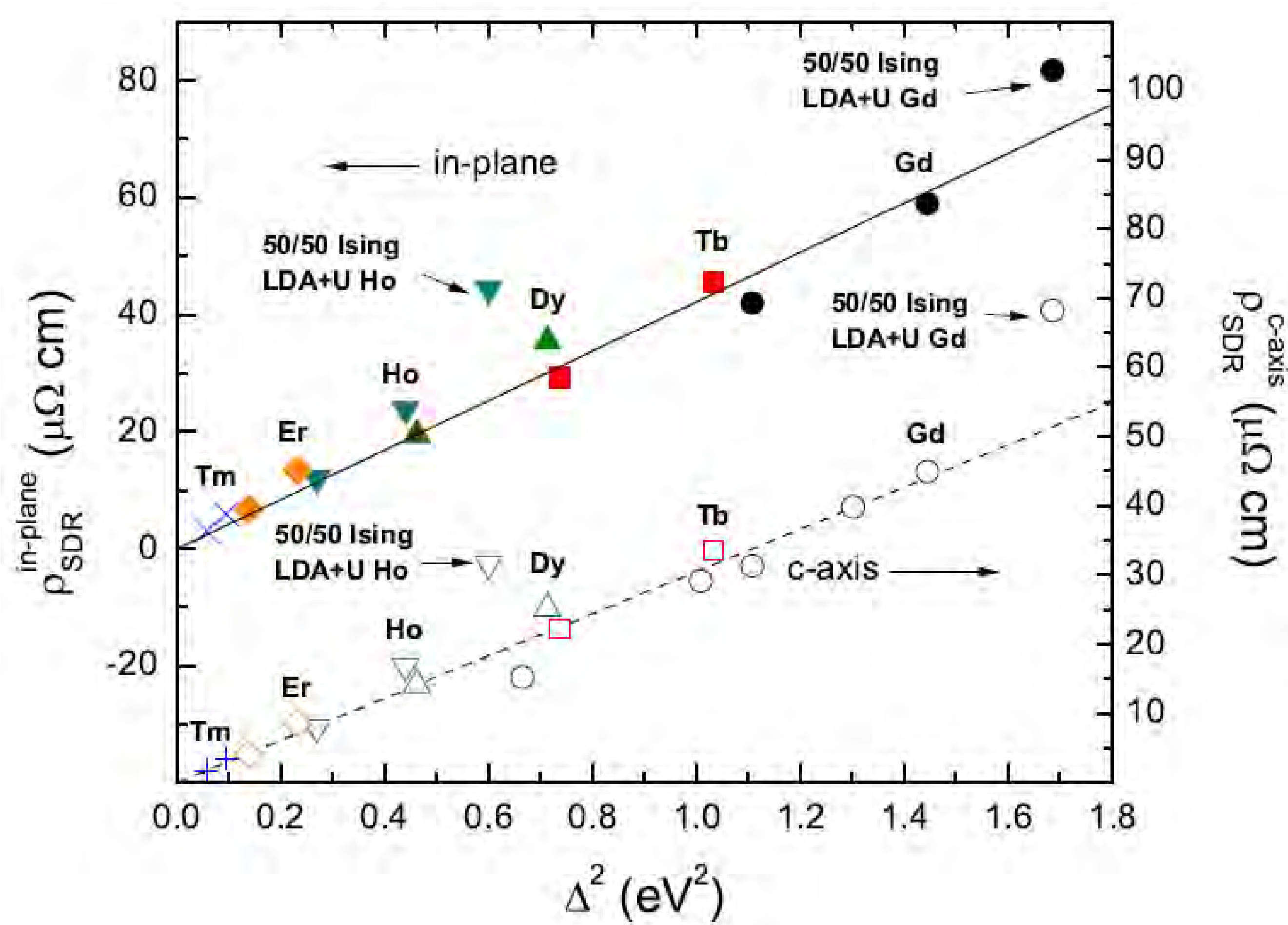

- Linear trend for both directions
- Larger *m* and ρ with 4*f* states treated using LDA+U

J. K. Glasbrenner, KB *et al.*, PRB 85, 214405 (2012)

Results (supercell and DLM methods)

LB = Landauer-Buttiker

Element	a, c	m, μ_B	In-plane			c-axis			Polycrystal		
			LB	DLM	Exp	LB	DLM	Exp	LB	DLM	Exp
Gd	6.858 10.952	7.72 7.44	58.9 42.0	59.1 40.2	108, 105[23]	44.9 31.3	41.5 26.9	96, 95[23]	54.2 38.4	53.2 35.7	106.4
Tb	6.805 10.759	6.64 6.35	45.6 29.1	46.0 27.7	82	33.5 22.2	30.2 17.6	66	41.6 26.8	40.7 24.3	85.7
Dy	6.784 10.651	5.58 5.27	35.4 19.4	35.3 18.6	62, 57[21]	25.1 14.1	22.6 11.7	44, 45[21]	32.0 17.6	31.1 16.3	57.6
Ho	6.760 10.612	4.46 4.20	23.8 12.0	22.8 10.8	41	16.8 7.93	14.3 6.8	24	21.5 10.6	20.0 9.43	32.3
Er	6.725 10.559	3.33 3.14	13.4 6.68	12.2 5.94	21, 32.4[25]	8.56 4.11	7.5 3.44	13, 18.0[25]	11.8 5.82	10.6 4.81	23.6
Tm	6.685 10.497	2.21 2.088	5.96 3.00	5.23 2.32	22.3, 21.2[24]	3.43 1.67	3.2 1.44	7.4, 9.0[24]	5.12 2.56	4.56 2.02	14.9

J. K. Glasbrenner *et al.*, PRB 85, 214405 (2012)

Exp. data: Legvold *et al.*, Maezawa *et al.*, Ellerby *et al.*

- CPA and supercell methods agree
- Anisotropy (ρ_c/ρ_a) grows with Z, well reproduced
- Magnitude is underestimated

Comparison with experiment, quantum corrections

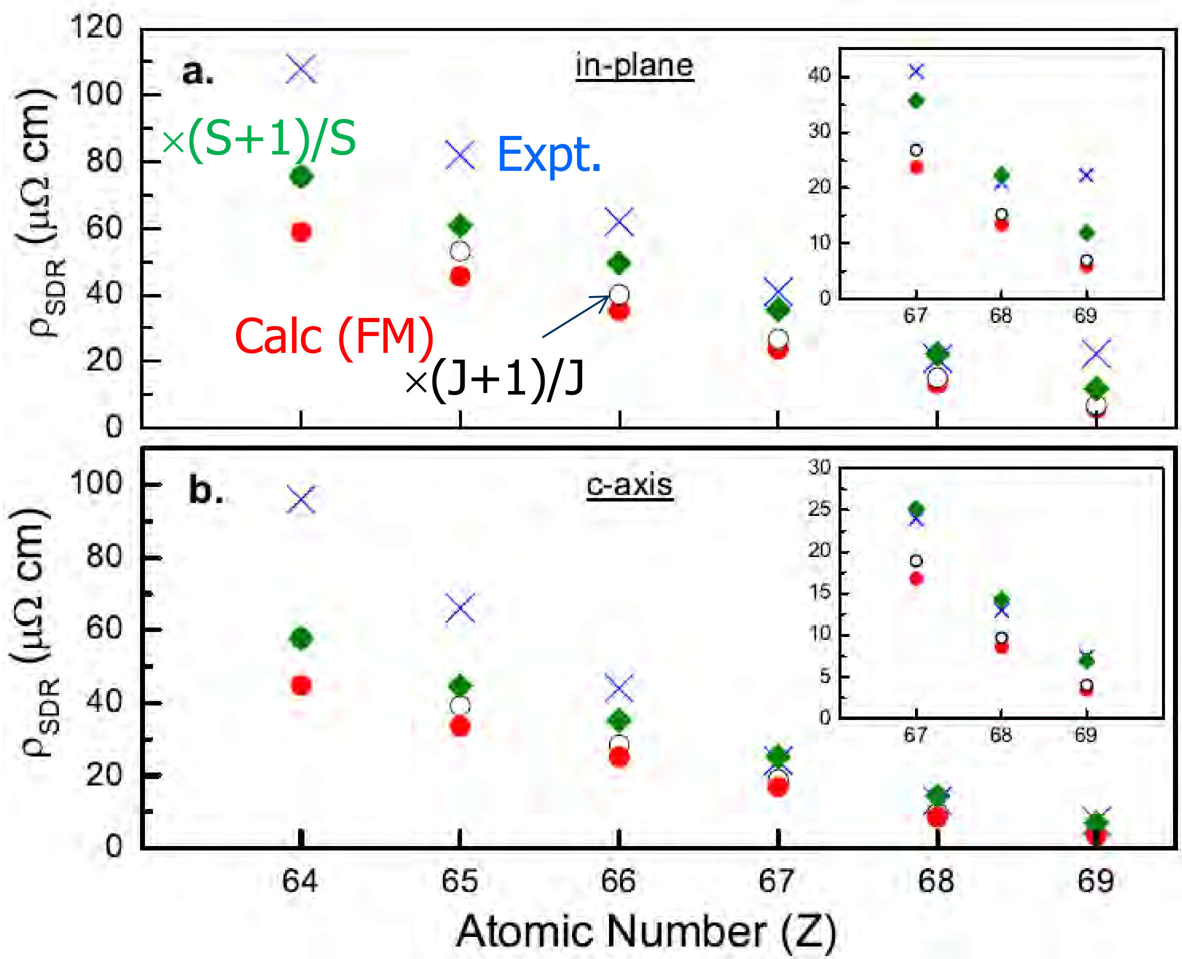

- Heavier elements: (S+1)/S correction improves agreement
- Lighter elements (Gd, Tb): large *S* and *J*, corrections too small
- Deviations from Matthiessen rule?

Combination of phonon and spin disorder

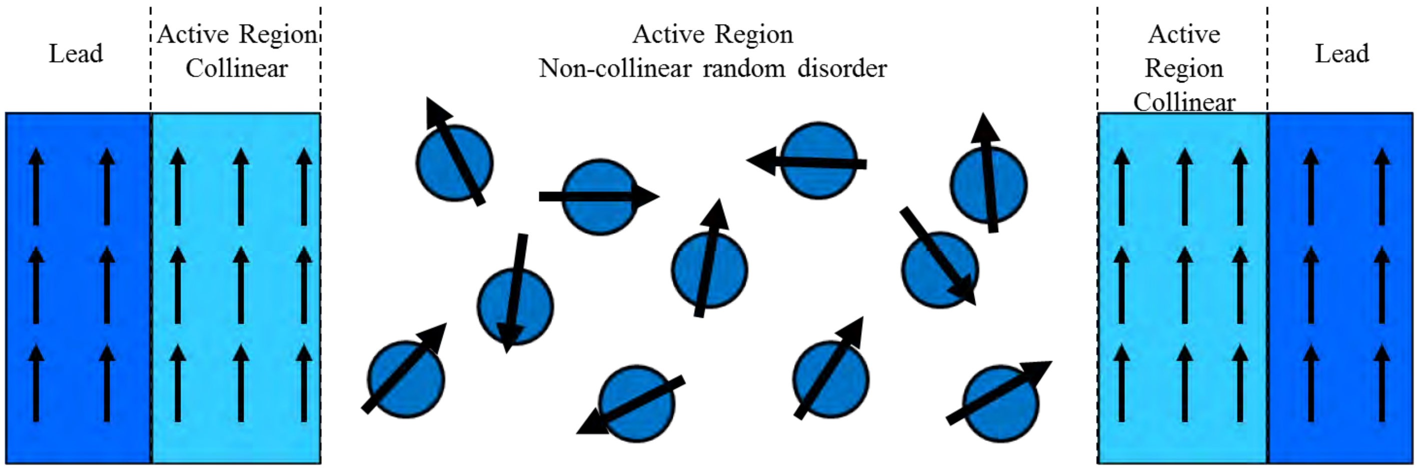

- Classical Einstein oscillator model

$$H = \frac{1}{2}k\mathbf{u}^2; Z = \int_{-\infty}^{\infty} e^{-H/k_B T} dx$$

$$\Delta_{ph}^2 \equiv \langle \mathbf{u}^2 \rangle \propto T$$

See also Liu et al., PRB 84, 014412 (2011)
(Gilbert damping)

Test for deviations from Matthiessen's rule:

- Maintain random spin disorder and add lattice displacements
- For independent phonon and spin scattering, expect $\rho = \rho_{\mathrm{SDR}} + \alpha\Delta_{ph}^2$

Resistivity crossover and "hidden" saturation in Gd

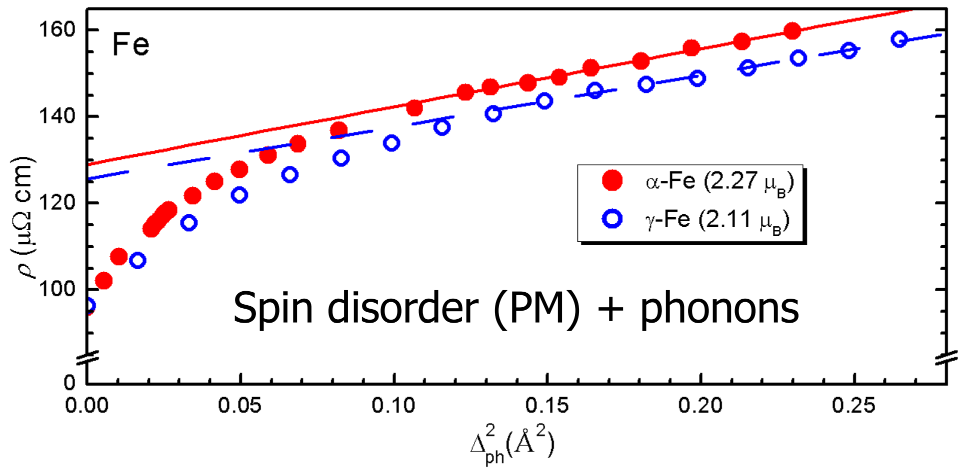

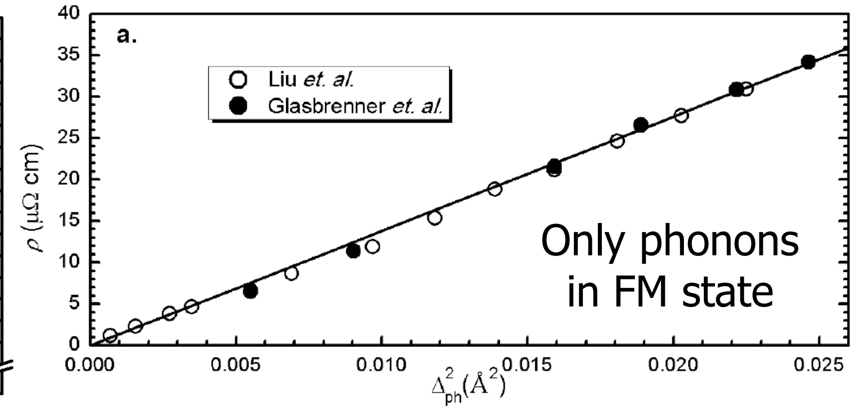

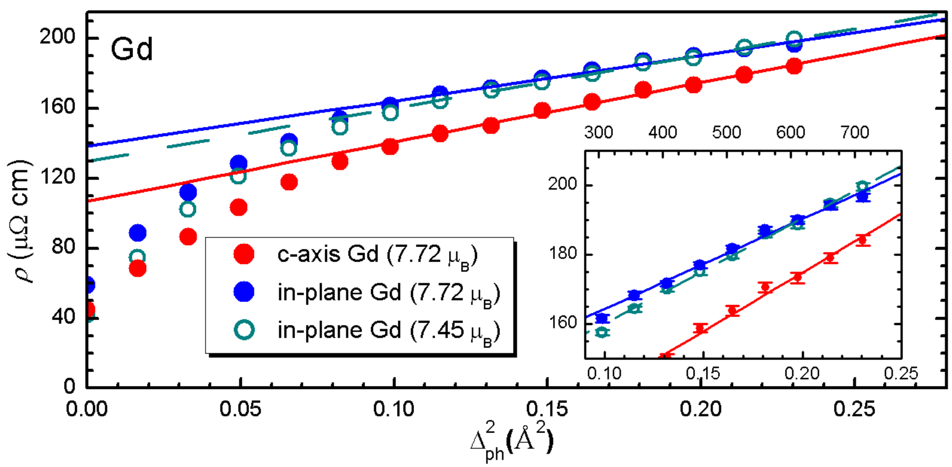

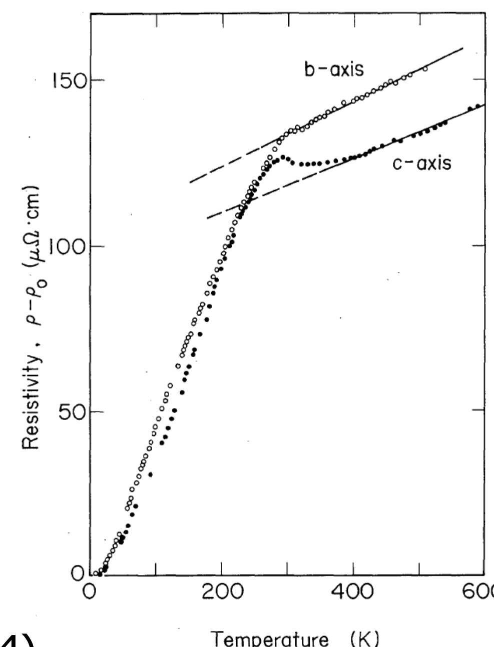

- "Hidden" resistivity saturation effect
- Violation of the Matthiessen rule

Glasbrenner *et al.*, PRB **89**, 174408 (2014)

Effect of Anderson disorder in Gd

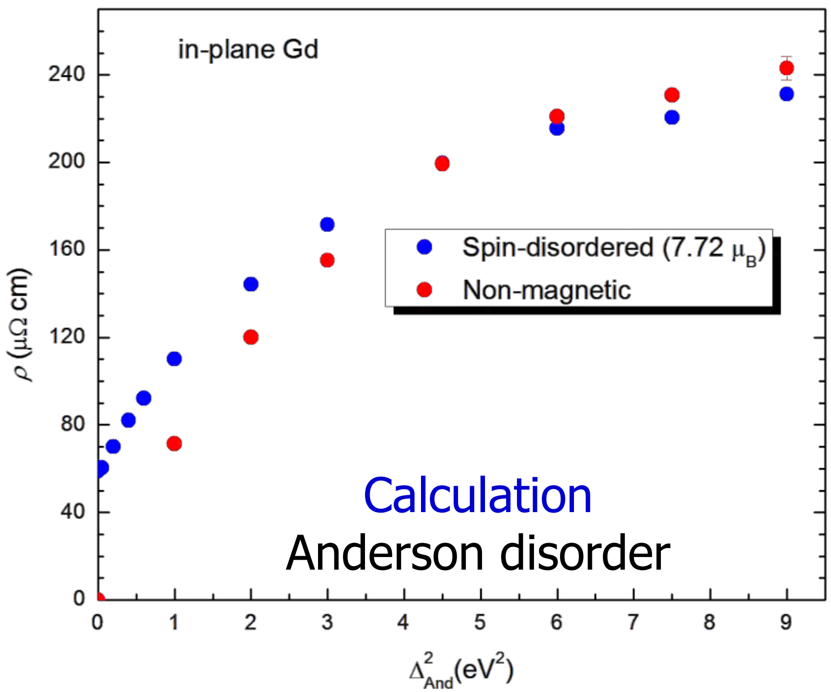

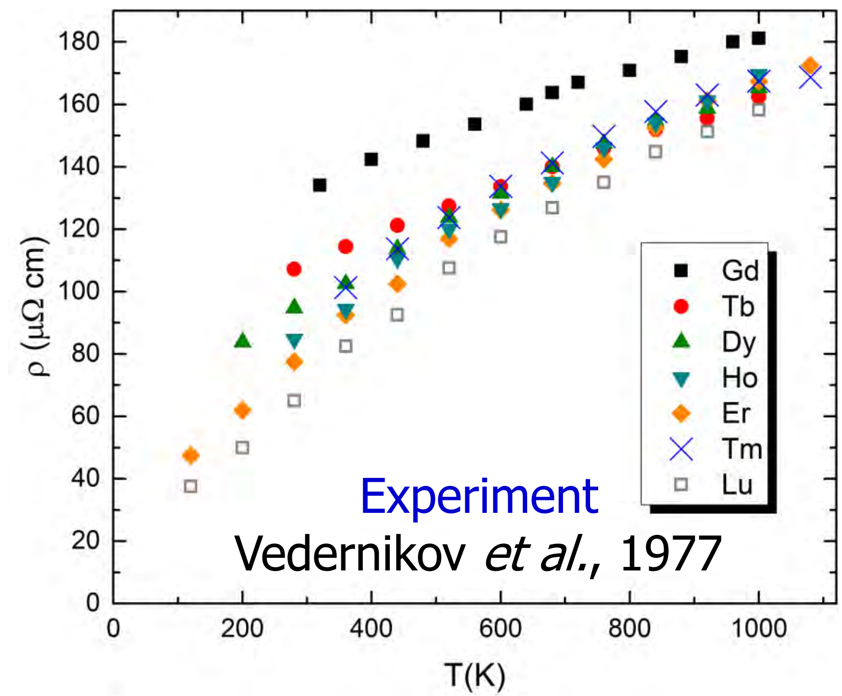

- Effect of Anderson disorder is similar to lattice displacements
- Resistivity saturation irrespective of the scattering mechanism
- Saturation trend in experiment

Spectral function of Gd:
Parts of Fermi surface destroyed by disorder

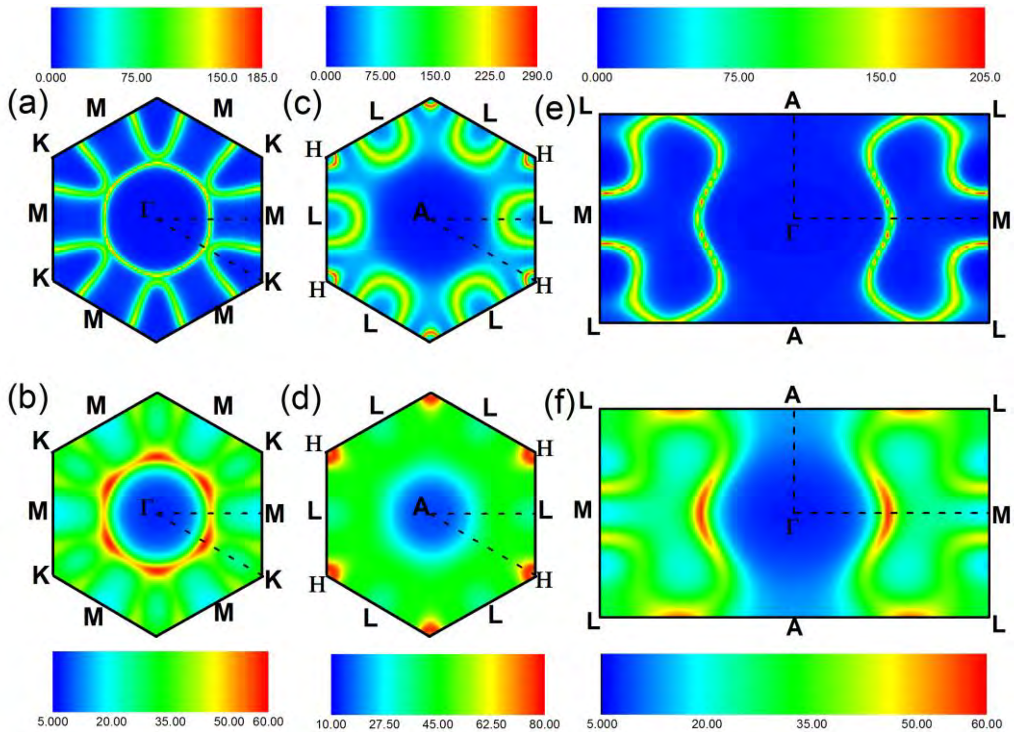

Δ=0

Δ=0.95 eV

Δ=1.8 eV

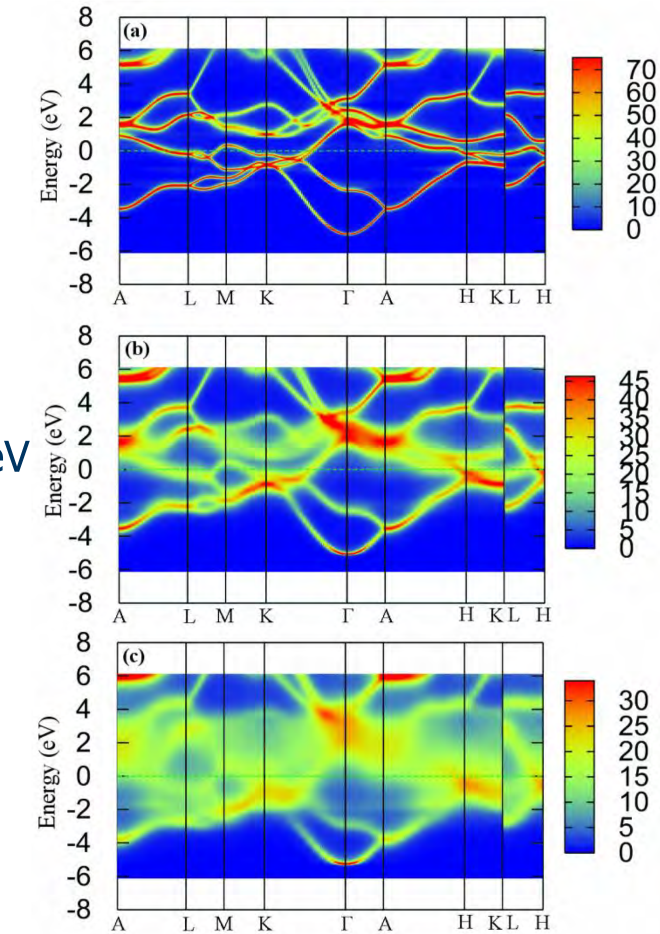

CPA-DLM + Anderson disorder

- ❖ Electron and hole-like Fermi surface sheets are degenerate on ALH plane
- ❖ Parts of Fermi surface are destroyed by disorder → resistivity saturation

Comparison with photoemission

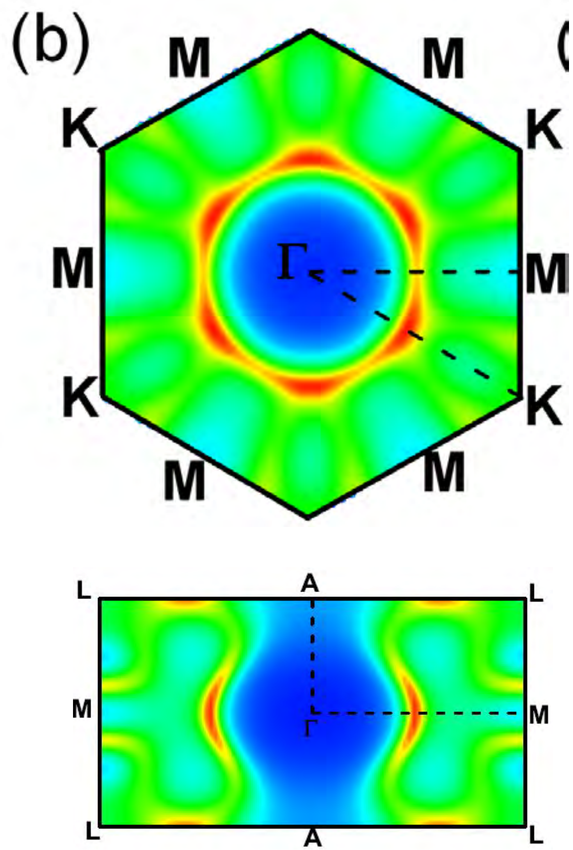

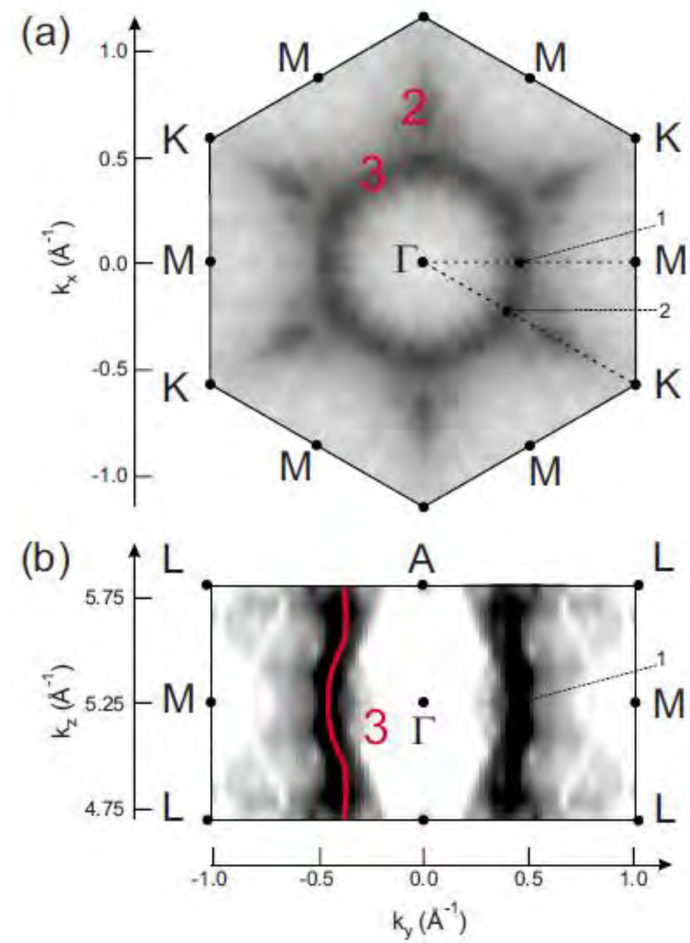

Döbrich *et al.*, PRB 81, 012401 (2010)
T = 300 K

Conclusions

- CPA-DLM treatment of spin fluctuations is a method of choice to study temperature-dependent electronic properties of magnetic alloys as long as dynamic correlations are irrelevant
- Implementation in TB-LMTO: vector DLM model with full charge self-consistency, constraining fields, total energy, spin-orbit coupling
- Anomalous temperature dependence of magnetic anisotropy in $(Fe_{1-x}Co_x)_2B$ is entirely due to spin fluctuations changing the electronic structure (band shifts and broadening)
- Strong thermal depolarization of half-metallic NiMnSb due to thermal spin disorder on Mn_{Sb} defects; testable dependence of the crossover temperature on Mn_{Sb} concentration
- Resistivity of Gd reinterpreted: collapsing parts of the Fermi surface and hidden resistivity saturation

Collaborators

Ivan Zhuravlev

Jeevaka Weerasinghe

Sai Mu (PhD 2014)

Bhalchandra Pujari

James Glasbrenner (PhD: UNL, now at NRL)
Vladimir Antropov, Liqin Ke (Ames)
Mark van Schilfgaarde (King's College London)
Josef Kudrnovský, Vaclav Drchal, Ilja Turek (Czech AS)
Sergii Khmelevskyi (TU-Wien)

Supported by NSF DMR-1005642, DMR-1308751, Nebraska MRSEC (DMR-0820521)